Edited by
Aleksander SŁADKOWSKI

FINITE ELEMENT METHOD FOR TRANSPORT APPLICATIONS

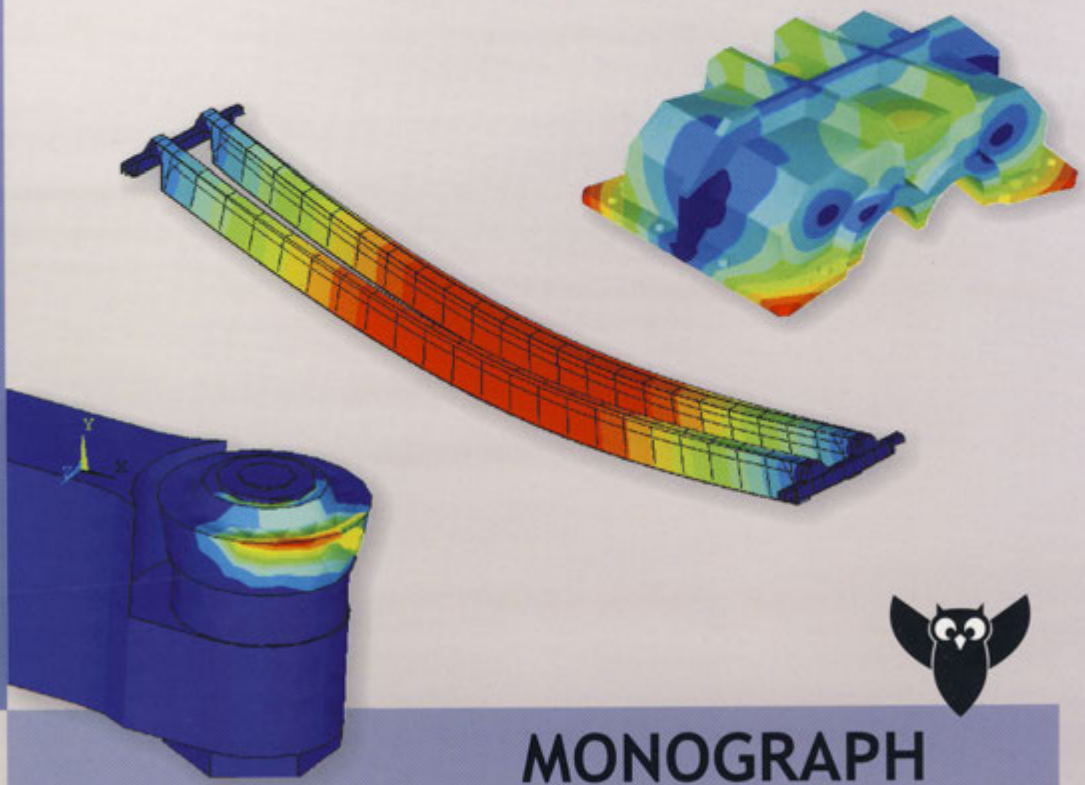

MONOGRAPH

WYDAWNICTWO POLITECHNIKI ŚLĄSKIEJ

GLIWICE 2011

Edited by

Aleksander SŁADKOWSKI

FINITE ELEMENT METHOD FOR TRANSPORT APPLICATIONS

SILESIAN UNIVERSITY OF TECHNOLOGY
GLIWICE 2011

Aleksander SŁADKOWSKI, Damian GĄSKA, Tomasz HANISZEWSKI[1]

FINITE ELEMENT METHOD USAGE IN DESIGNING TRANSPORT MACHINERY AND MATERIAL HANDLING EQUIPMENT

1. USING OF THE FEM FOR ANALYSIS OF INDUSTRIAL TRANSPORT PROBLEMS

Designing of machines for material handling (industrial) requires from the designer application of fast and accurate computational methods. The result of such process should be a design of structures that are reliable in operation, fulfil the conditions of strength, and cost-effective in case of materials. This is achieved through the use of computer aided design system, the integrated CAD/FEA applications.

Computational model of structure should reproduce all the important parameters and factors affecting to the behaviour of the structure in question of the ultimate limit state, namely: the load and impact of material properties, geometrical features and stiffness characteristics (susceptibility) of elements, stiffness of mergers and concentrators [1]. In order to reliably mapping the actual behaviour of structure in computer simulations, many factors must be taken into account. The inclusion of too many degrees of freedom, leads to a very sophisticated model, which solution by numerical methods may cause certain difficulties. Therefore, conducting research on virtual numerical models, there is a need to find a compromise between efficiency and accuracy of performed calculations. Making simplifications, the establishment of boundary conditions and appropriate mesh of finite elements is one of the most difficult and important tasks that must be carried out during computer simulations.

In the era of computerization, tools that help design engineers in work are integrated CAD/FEA applications. Software for computer-aided design – CAD systems – allows execution in a short time, the 3D geometric model, and thanks to the advantages of FEM applications (Finite Element Method) model can be analyzed in a short time to verify for strength for certain boundary conditions. Such flow diagram is used when designing transport machinery and handling equipment.

Transport machines and handling equipment are primarily passive and active means of transport used within the company area. These are all types of lifting equipment – cranes, conveyors, forklifts and mobile, as well as passive means of transport in the form of pallets, racks, etc.

2. DESIGN METHODOLOGY FOR 3D MODEL USING AUTODESK INVENTOR

Autodesk Inventor provides a comprehensive and integrated set of applications and tools for converting 2D data to facilitate the transition to 3D design system, includes Autodesk Inventor – for 3D design system and creating technical drawings, AutoCAD Mechanical for 2D drawing creation and Autodesk Vault for data management [2].

[1] Silesian University of Technology, Poland

Autodesk Inventor is an advanced solid – surface modeler, which is used to design the device as a 3D model, then generate on its basis assembly drawings, production drawings, regulations, bidding, and illustrative. Any changes made in the model are automatically included on all drawings, by using the full parameterization of the model, additional dimensional and standards data can be linked to the Excel spreadsheet. The software allows to create its own library of parametric parts, so it is easy to create a library of parts which are unique and widely used in current projects [3].

Autodesk Inventor also delivers a completely new, created from scratch, modeling paradigm - functional design. This approach to design allows designers to move beyond geometric modeling and enter into the environment in which the engineer can focus on solving the problems of design, rather than spending time on creating 3D geometry required to create a project [2].

2.1. Fundamentals of project management

The program allows to manage the project structure in a very simple way, through the use of manual systems. A typical multi-access avoids the risk of deleting legitimate files. The basic principle of organization: files (see fig. 1) are organized into projects, each project must have a unique name, and should have a defined workspace.

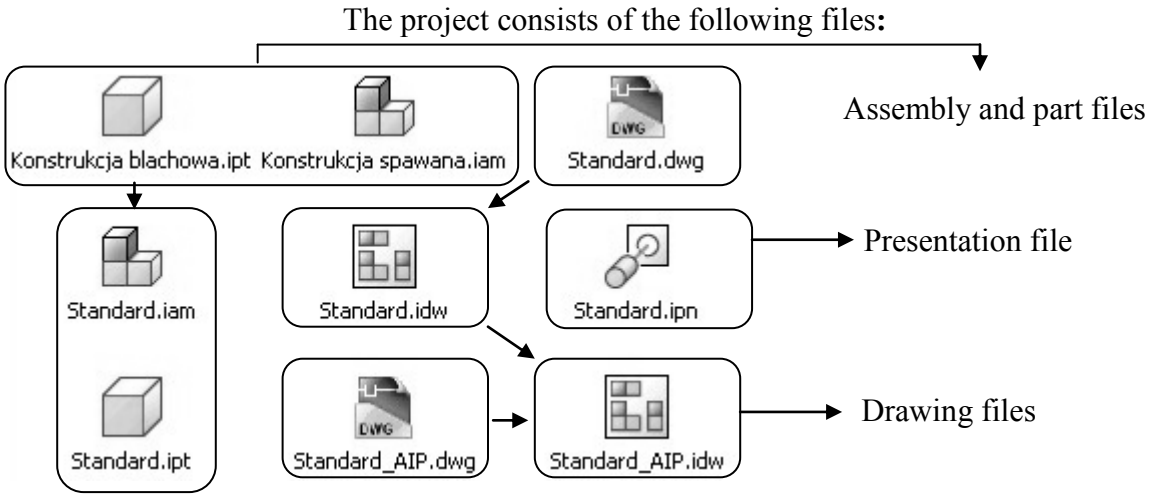

Fig. 1. The types of files in the project
Rys. 1. Rodzaje plików w projekcie

2.2. The process of 3D model building

Creating a 3D model consists in the most general case of several steps, shown in fig. 2 [4]:

With a full parameterization in Autodesk Inventor, it is possible to modify existing drawings and operations, each change is automatically recorded and entered, so you can quickly modify the design even in its final phase.

2.3. 2D sketches, 2D operations

The process of creating a sketch and the establishment of operations in the Autodesk Inventor software does not differ from the conventional process of drawing in a 2D AutoCad programs, if necessary, the program has an extensive library which help in most cases and is able to replace the book. In case of problems Autodesk team is happy to provide assistance to students belonging to the Autodesk Student Community. It is a community consisting of a group of students from around the world, membership is free and students can use the whole range of Autodesk products.

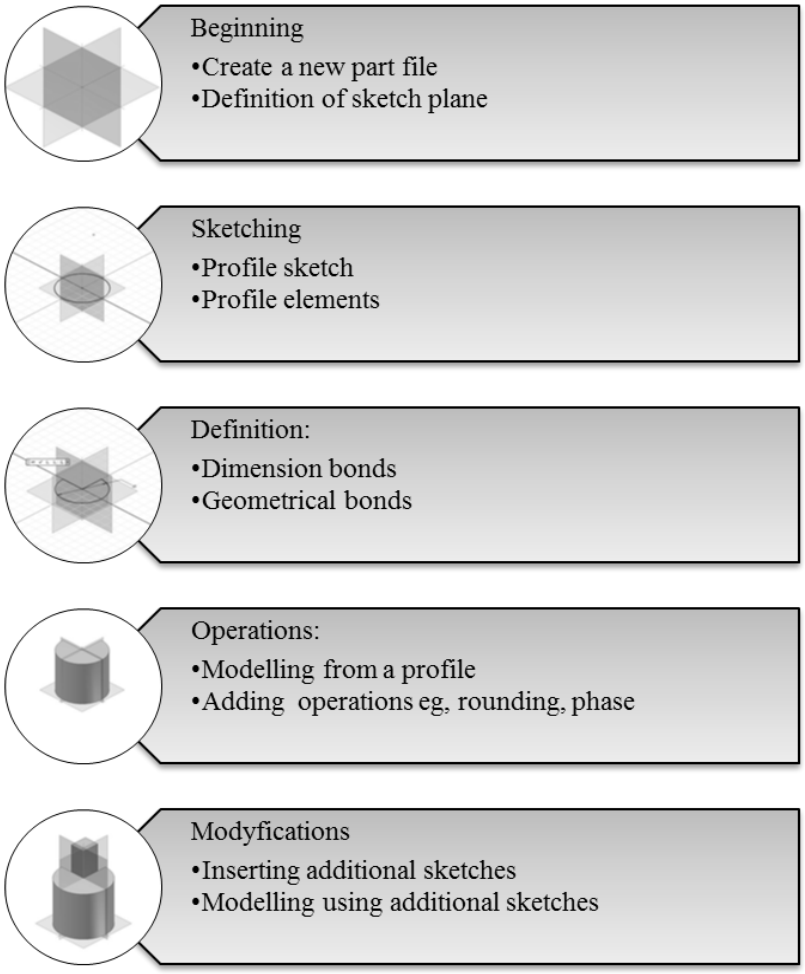

Fig. 2. The process of 3D model building
Rys. 2. Proces tworzenia modelu 3D

2.4. Assembly creating, 3D operations

With the submission of finished components (separate files) it is possible to go to their so-called virtual assembly. To do this, creation of a file submission is needed. Then insert all the necessary components and specify 3D operations (fig. 3).

Through the use of assembly operations, it is possible to make the parts into assembly, each of the operations also can be given a numerical range corresponding to the possibility of: trading or offset against each other, which is useful when creating assembly animation. The module "assembly" also contains additives in the form of cable insertion, standard parts, pipelines and bolts which are significantly simplifying the job. One interesting feature is

called Design Accelerator which allows to create the fundamental parts of machinery such as shaft and make basic calculations. Sample shaft is shown in fig. 4.

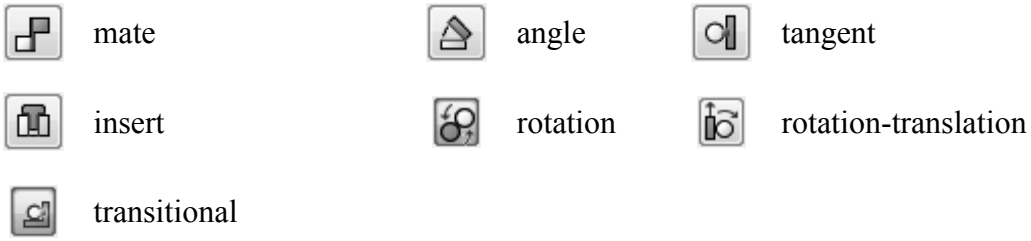

Fig. 3. Types of operations
Rys. 3. Rodzaje więzów

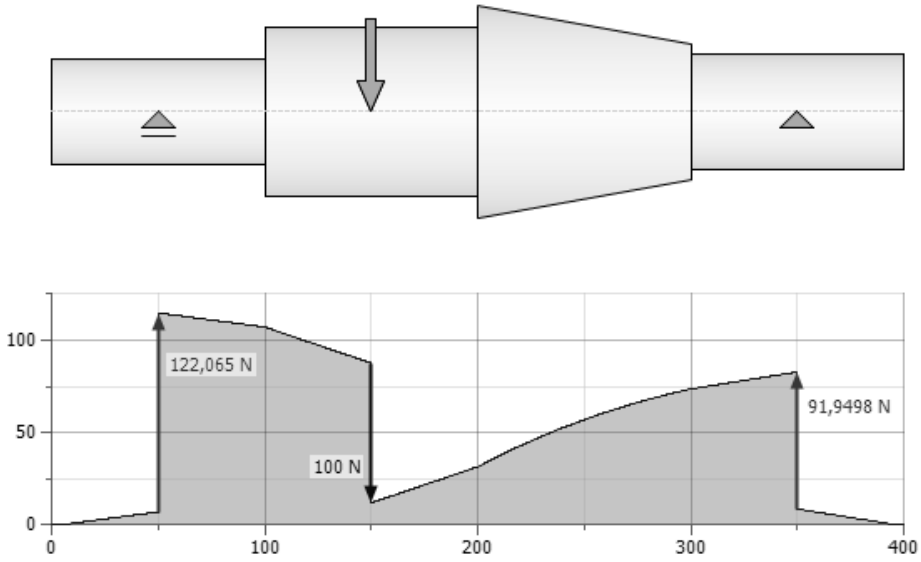

Fig. 4. Sample shaft in module Design Accelerator
Rys. 4. Przykład projektowanego wałka w module Design Accelerator

2.5. 2D documentation

Drawing environment allows to create drawing views of parts and assemblies, and then adding their descriptions. Drawings needed to guide the production of the mechanical part or assembly are printed or plotted. Changes to component or assembly are automatically updated in the drawing views.

Types of view that can be created in the drawing environment:

- base view: first created view, all other views are created based on this one;
- projection views: orthogonal or isometric projection, formed on the basis of the base view or another existing view;
- auxiliary views: a view perpendicular to the selected edge or line;
- sectional views: the view formed by the intersection of the plane or assembly, view represents an area of the surface intersection;
- detail: enlarged view of a portion of a different view of the drawing, details allow to add a clearer and more detailed descriptions;
- sketched view: a view that contains one or more associated 2D sketches (fig. 5). Such views are not created from three-dimensional parts [5].

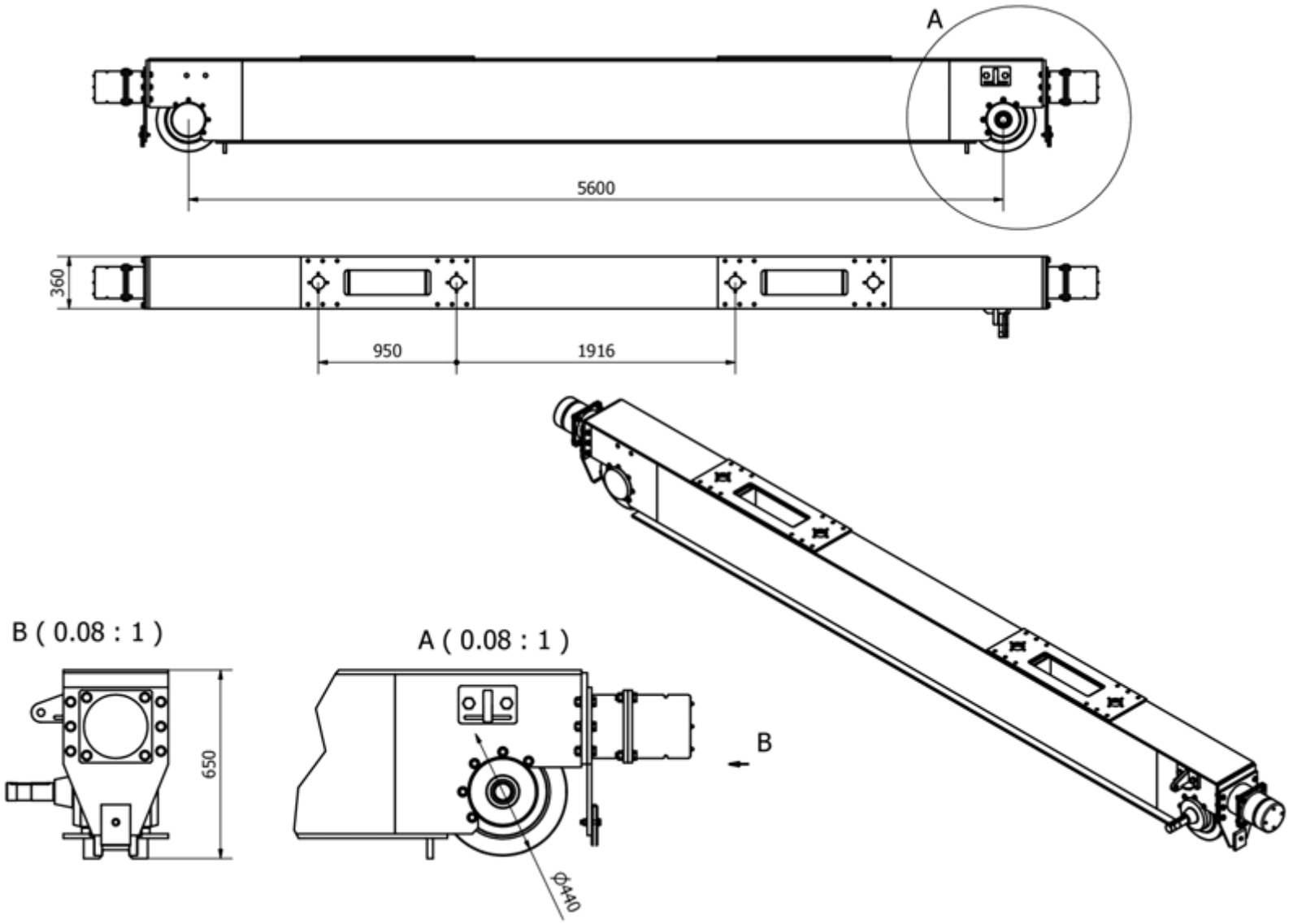

Fig. 5. 2D documentation
Rys. 5. Dokumentacja 2D

2.6. Realistic model presentation

By using Inventor Studio it is possible to create realistic renderings of created model and animation, as well as a detailed view, that not once is invaluable when creating documentation. An example of the process of creating 3D presentations are shown in fig. 6.

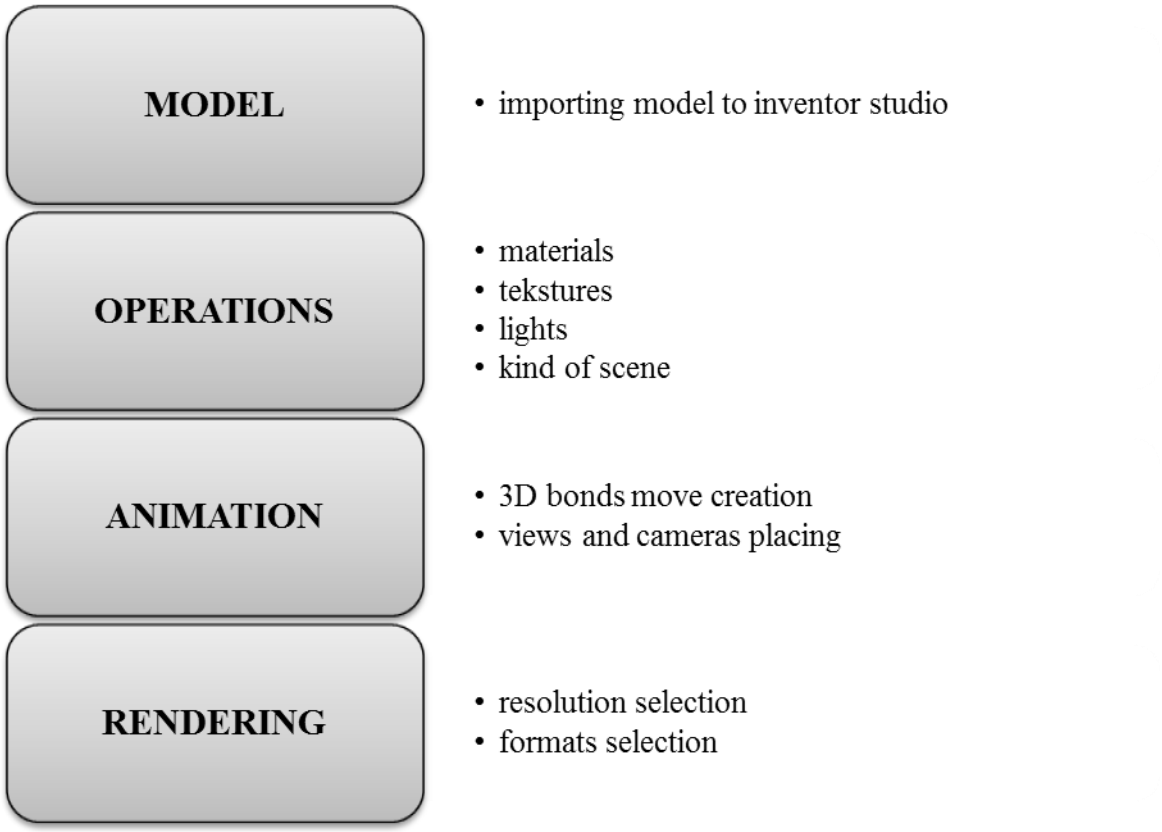

Fig. 6. 3D presentation creating process
Rys. 6. Proces tworzenia prezentacji 3D

Below is an example of rendering the open side of the cranes buffer beam and the detailed drawing (fig. 7, 8).

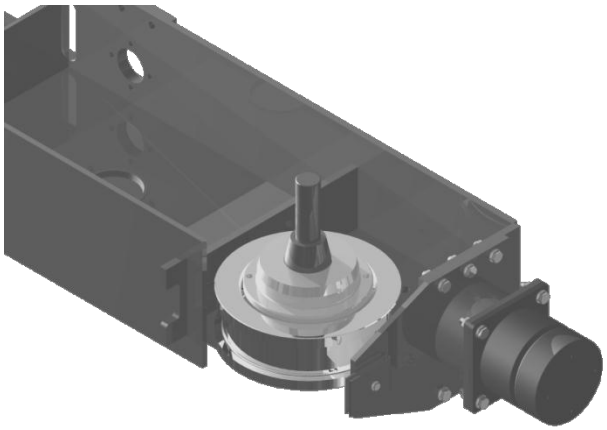

Fig. 7. Rendering of the model
Rys. 7. Rendering modelu

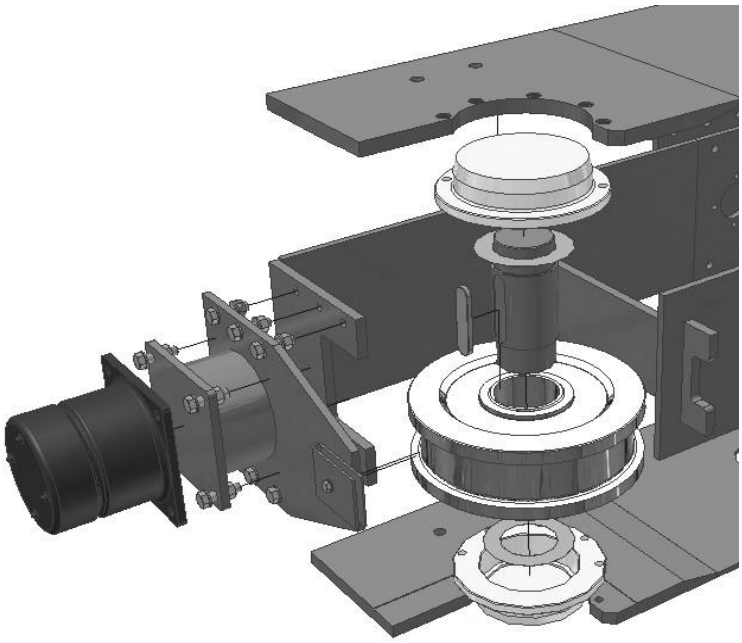

Fig. 8. Presentation of detailed 3D model
Rys. 8. Prezentacja widoku rozstrzelonego 3D

2.7. The methodology of the FEM model creation, the definition of the problem on the example of the crane bridge

Computer software implementing itself the finite element method, consists of three main modules:

- **pre-processor**: creation of FEM model (boundary conditions, material…)
- **processor**: calculation module;
- **postprocessor**: graphical results presentation and its analysis.

An example of the process of creating a task for FEM is shown below:

- importing geometrical features to pre-processor;
- preparing the geometry for the imposition of FE mesh;
- FE mesh creation;
- boundary conditions;
- loads, mass, kinematical loads…;
- the creation of sets of nodes and elements;
- assigning section to the sets of elements;
- export to a batch file.

2.7.1. FEM model, pre-processor

Analyzed load-carrying structure is a construction of overhead crane (fig. 10) [6], in which one dimension (thickness) is significantly smaller than the other. Such a system is often called the box-girder, which is characterized by a high load capacity. Surface structure is limited by the top, bottom and side surface. The example is shown in fig. 9 [1, 7].

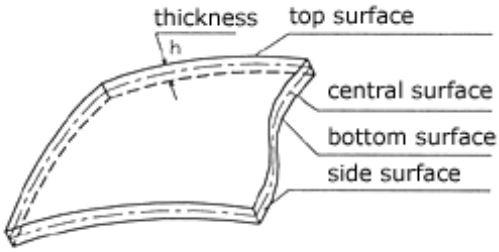

Fig. 9. Surface example
Rys. 9. Przykład powłoki

In the truss frames rods are replaced by their axes, in the case of the box girder by the middle surface parallel to the upper and lower one, where the thickness is the smallest dimension measured along a straight line normal to the middle surface, between upper and lower one. System in which the surface is a plane is called "plate" and "shell" when the surface is curved, in the present structure are both plates and shells [7].

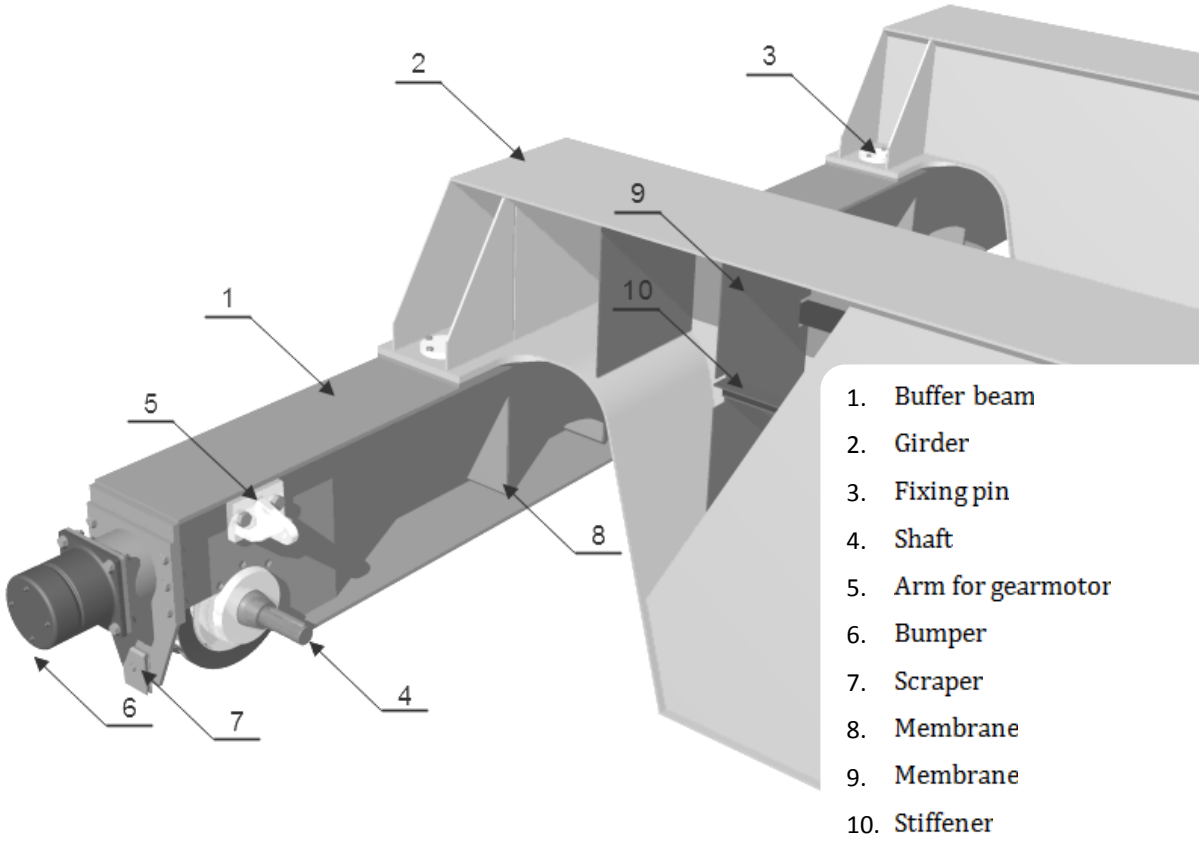

Fig. 10. Cranes load-carrying structure
Rys. 10. Ustój nośny suwnicy

The first step in creating an FEM model is to simplify the geometry, consisting of getting rid of certain parts of the structure, such as bolted joints, wheel sets. Then using the preprocessor of the surface model middle surfaces are isolated where the FEM mesh will be created. However, it is necessary to improve the so formed surface, as a result of the philosophy of creating middle surface. The middle surface before the improvements is shown in fig. 11.

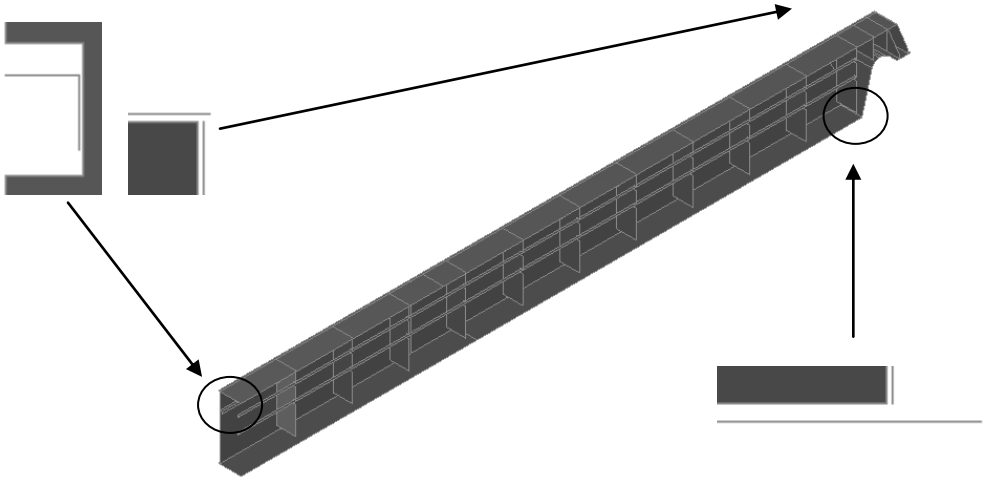

Fig. 11. Middle surface
Rys. 11. Powierzchnia środkowa

The quickest solution is to export such a formed surface back to Inventor, improve and re-export to the preprocessor. After preparing the middle surface, the shell elements mesh was made of (PSHELL) TRIA and QUAD-type 4 and 3 nodal, in size of 40 [mm]. In this way a mesh made of 269694 elements was obtained. Elements have been given the proper thickness of sheet steel in the structure corresponding to the load-carrying crane structure. Fragment of the model is shown in fig. 12.

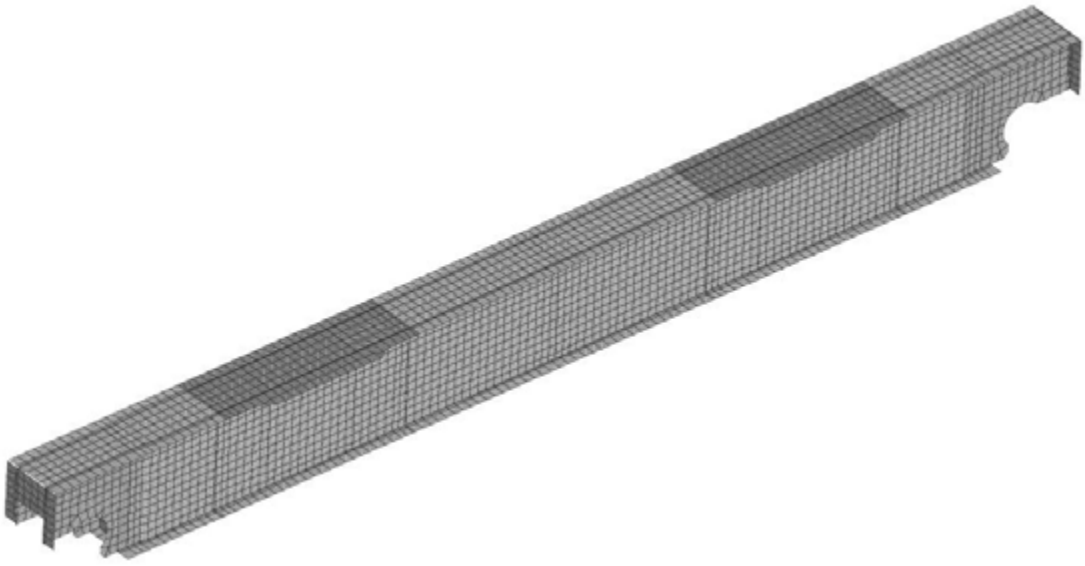

Fig. 12. FE mesh of load carrying crane structure fragment
Rys. 12. Widok siatki elementów skończonych fragmentu suwnicy

2.7.2. Boundary conditions

In order to simplify the model, instead of modeling power trains, structure was restrained as shown in fig. 13. Using the element type RIGID (RBE2), restrain was transferred from the points on the drive shaft axle to the buffer beam structure.

In the place of fixed support was fixed all six degrees of freedom. On the other side of the load-carrying system only two degrees of freedom were taken away: a shift in the X-axis (the

direction of motion of the bridge) and the Z-axis (perpendicular to the plane XY) - because the crane can move along the axis perpendicular to the axis of motion of the bridge, due to loads caused by skewing.

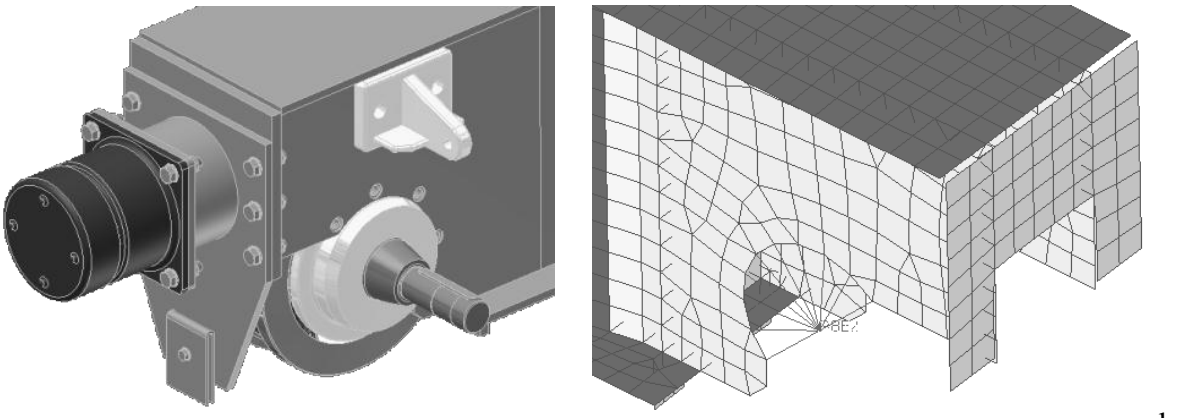

a b

Fig. 13. Fixed support: a) Real model; b) Simplified model for calculations purposes
Rys. 13. Utwierdzenie: a) model rzeczywisty; b) model uproszczony dla celów obliczeń

For loads application that is acting on load-carrying system, it is essential to modeling the rails on which the trolley (crane winch) is moving. The rail was simplified to the bar element, modeled as CBAR. This element was assigned a number of properties, such as:

- moments of inertia with respect to x and y axes;
- the principal moment of inertia;
- material;
- transverse surface area;
- mass per length unit.

Thanks to this type of modeling real rail was imitated. Elements used are presented in fig. 14. Using CBAR elements in the model increasing the stiffness was incorporated, which usually introduces a rail welded to the upper flange of girder.

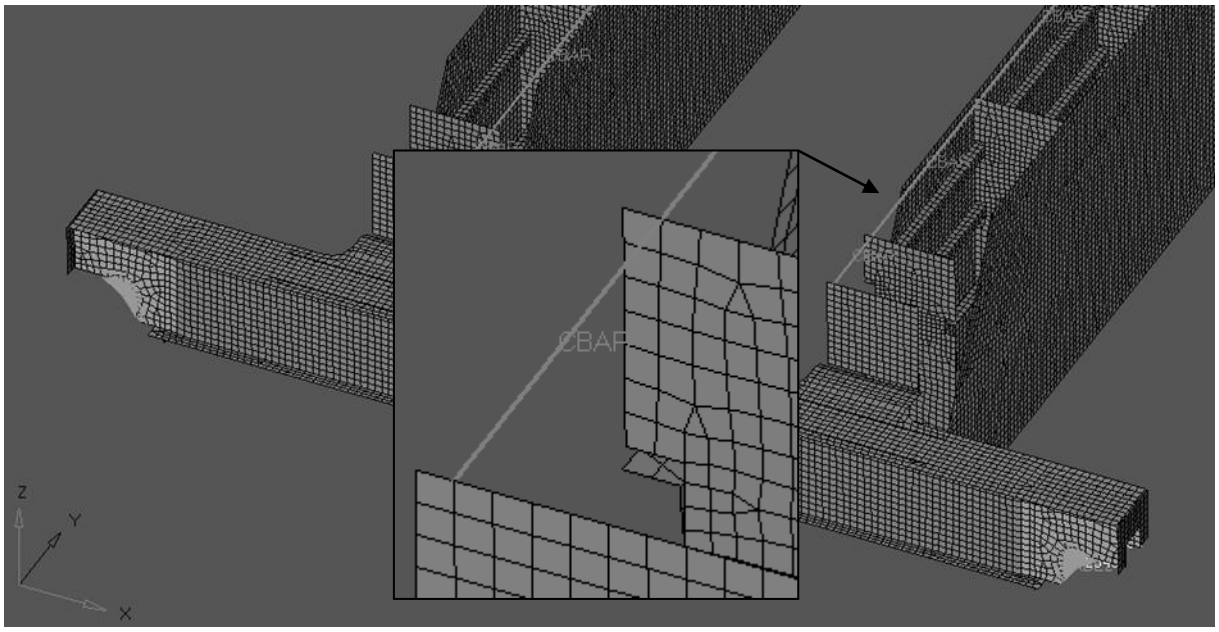

Fig. 14. CBAR elements usage in rail modelling
Rys. 14. Zastosowanie elementu CBAR w modelowaniu szyny

2.7.3. Loads application and setting of material

Loads resulting from the crane load were applied in the points of the wheels of the trolley contact with rail of overhead crane. Ultimately, three extreme positions were selected, the centre and ends of the girder. The method of application is shown in fig. 15.

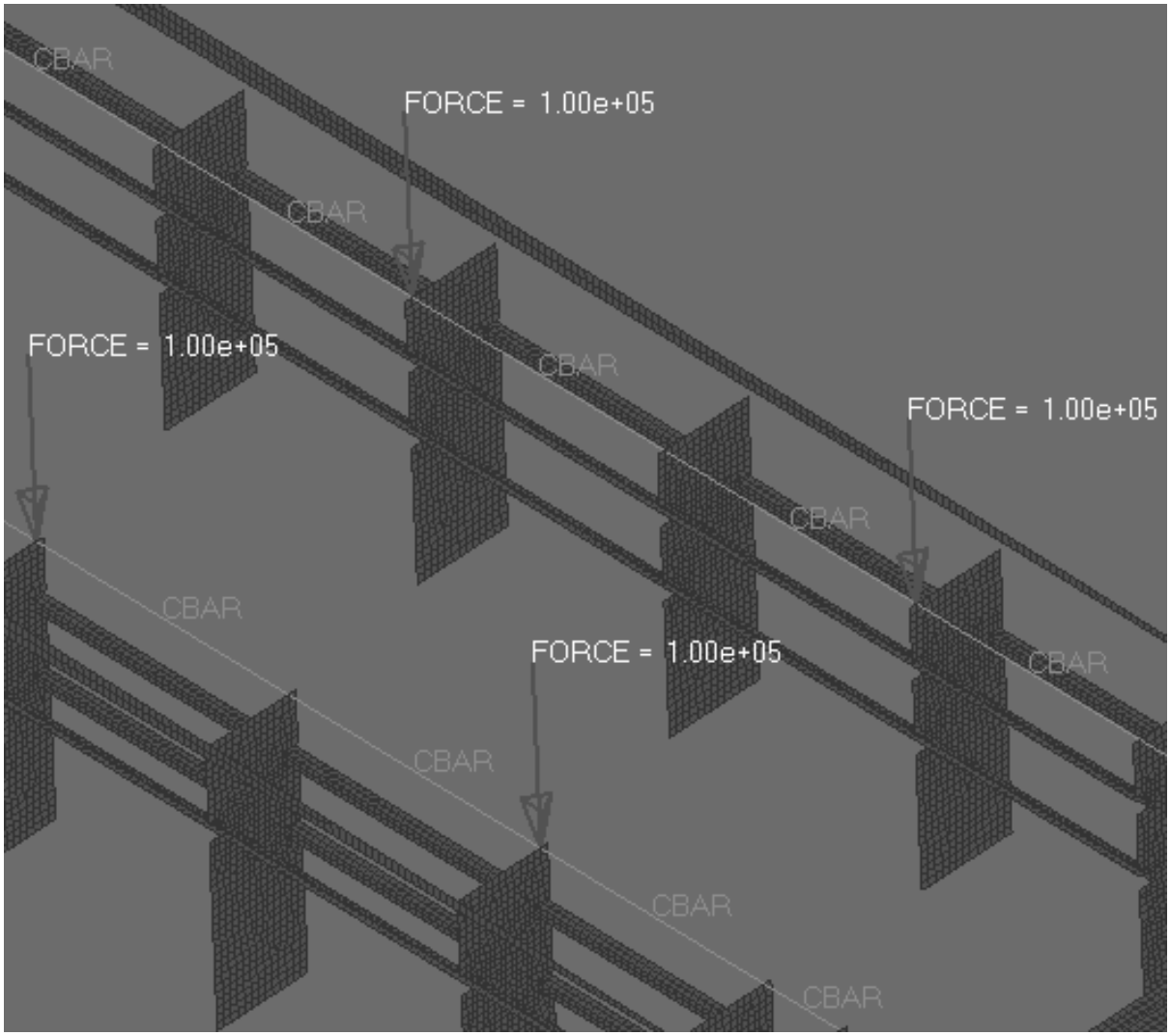

Fig. 15. Loads application
Rys. 15. Przyłożenie sił

The material from which the crane structure is made is stainless steel, and therefore for the purpose of the calculation such material properties were applied:

- Poisson ratio $\nu = 0{,}3$;
- Young's modulus $E = 210000[MPa]$;
- density $\rho = 7{,}85 \cdot 10^{-9} \left[\frac{ton}{mm^3} \right]$.

Such specific units results from the adoption [N] as a basis for the calculation of force and [mm] for distance units. For illustrative purposes, a coherent system of units for FEM is shown in table 1.

Table 1

Coherent system of units for FEM

	Mass	Length	Time	Load	Stress	Steel density	Young's modulus for steel	Gravity
1	kg	m	s	N	Pa	7850	2,05e+11	9,81
2	kg	m	ms	MN	MPa	7850	205000	9,81e-06
5	kg	mm	s	N*e-3	kPa	7,85e-06	2,05+08	9,81e+03
6	kg	mm	ms	kN	GPa	7,85e-06	205	9,81e-03
7	ton	mm	s	N	MPa	7,85e-09	205000	9,81e+03
8	ton	mm	ms	MN	TPa	7,85e-09	0,205	9,81e-03
9	ton	m	s	kN	kPa	7,85	2,05e+08	9,81e+00
10	ton	m	ms	GN	GPa	7,85	205	9,81e-06

The final step in preparing the model for the calculation is to create a schedule, or what steps PROCESSOR should made to perform calculations. In the case of Nastran there are so called LOADSTEPs in which interesting calculations are selected. Sample LOADSTEP for determining the stresses and displacements, for the nominal load located in the middle of the girder is shown in table 2.

Table 2

Sample LOADSTEP for NASTRAN processor

```
LOADSTEP          1"Obciazenie_20_T"
SUBCASE     1
 LABEL=   Obciazenie_20_T
 LOAD =      5 (load identification number)
 SPC  =      4 (restrain identification number)
 ANALYSIS = STATICS (static analysis)
 DISPLACEMENT(PLOT) = ALL (displacement calculations)
 STRESS(PLOT) = ALL (stress calculations)
 STRAIN(PLOT) = ALL (strain calculations)
```

In addition an application of gravity forces was used. Making a calculation taking into account the gravity is reduced to the introduction of the statement with a parameter value equal to the gravitational acceleration multiplied by the coefficient of dynamic loads in value of 1,22 [acc. to 19], that's why gravity factor was 11968,2.

Table 3

LOADSTEP for gravity force

```
LOADSTEP          2"Grawitacja"
SUBCASE     2
 LABEL=  Grawitacja
 SPC  =      4
 LOAD =      3
 ANALYSIS = STATICS
 DISPLACEMENT(PLOT) = ALL
 STRESS(PLOT) = ALL
 STRAIN(PLOT) = ALL

LOADCOL           3"grawitacja"
GRAV        3       11968.0 0.0     0.0     -1.0 (direction of gravity force)
```

Loadstep that combines loads and gravity effects is shown in table 4.

Table 4

Hoisting load and gravity effect combination

```
LOADSTEP          3"Obciazenie_Masa_Wlasna"
SUBCOM      3
  LABEL= COMBINE SUBCASES 1 AND 2
  SUBSEQ = 1.0,1.0
  ANALYSIS = STATICS
  DISPLACEMENT(PLOT) = ALL
  STRESS(PLOT) = ALL
  STRAIN(PLOT) = ALL
```

Such prepared model is being exported to execute file of PROCESOR. For example, this may be one of the few extensions: *.nas or *.dat.

2.7.4. Calculations – processor

In calculations as processor the MSC/NASTRAN was used. It is software that solves complex engineering problems using finite element method. It is widely used in engineering and the automotive, aerospace, shipbuilding, steel and mining industry.

With use of MSC/NASTRAN such engineering problems can be solved:

- Linear Static
- Modal
- Buckling
- Non-Linear Static
- Direct Complex Eigenvalue
- Direct Frequency Response
- Direct Transient Response
- Modal Complex Eigenvalue
- Modal Frequency Response
- Modal Transient Response
- Nonlinear Transient
- Static Aeroelastic Analysis
- Flutter / Aeroservoelastic analysis
- Dynamic Aeroelastic Analysis
- Non-Linear static coupled with heat transfer
- Nonlinear Transient coupled with Heat transfer
- Design Optimization and Sensitivity analysis
- Non-Linear Static and Dynamic (implicit) [8].

2.7.5. Analysis of results: stress distributions

Using the crane model 3 kinds of simulations was made: assuming no load (just own weight), the nominal load and nominal load in the two extreme positions (excluding the weight of its own).

In the absence of a load acting on the load-carrying structure, the greatest stress was 102 [MPa], and the maximum deflection 21 [mm]. As shown in fig.16 the maximum value occurs at a node located on the buffer beam around wheel shaft impact on structure, this value may result from the excessive rigidity arising from the support modeling process.

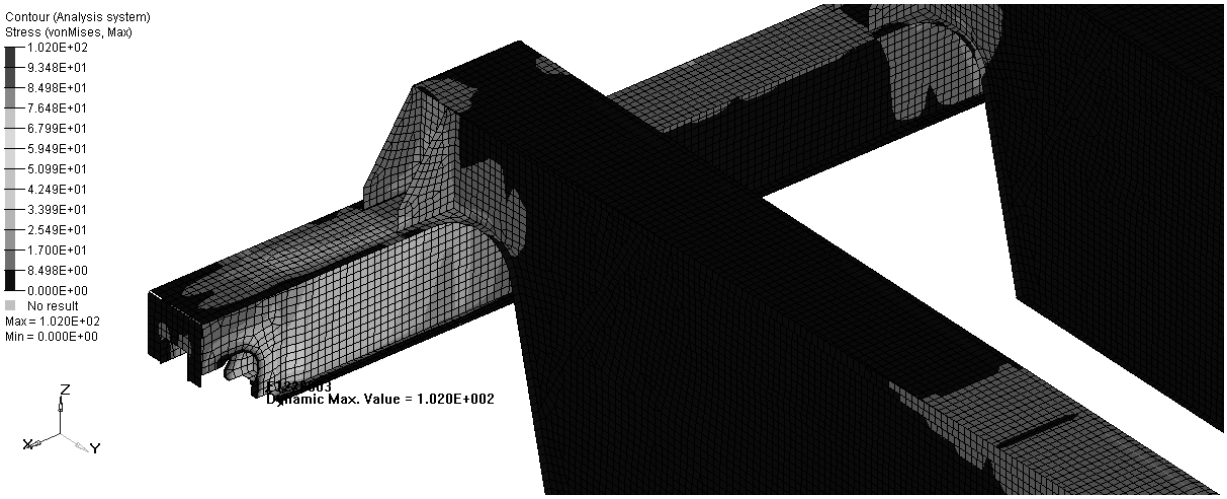

Fig. 16. Stress due to the own mass of structure
Rys. 16. Naprężenia wywołane masą własną ustroju

In the case of nominal load – 200 [kN] in the middle position of the girder, the greatest stress was 105 [MPa], and the maximum deflection 17,5 [mm]. As shown in fig. 17 the maximum value occurs at a node located on the girder in place of force, because the forces are applied at points stress value may be slightly higher than the actual.

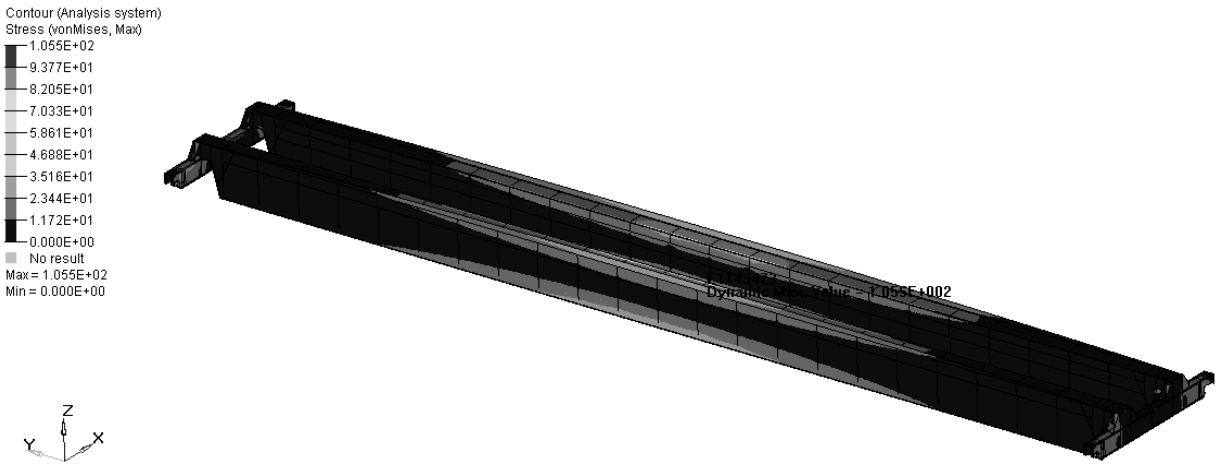

Fig. 17. Stresses due to the nominal load
Rys. 17. Naprężenia wywołane masą ładunku

The case of combination of nominal load and own mass (gravity effect) is shown in fig. 18, where f is maximal allowable deflection and L is crane span.

According to table 5 [9] for a double girder crane in question (the hook one) with a length of 34,5 [m] – limit value should be within: $0{,}001 \leq 0{,}0011 < 0{,}00125$. Stress value is 165 [MPa] (fig. 18) and the deflection 38 [mm] (f/L = 0,0016), which, according to the standards guidelines, is located in the predicted boundary.

Table 5
Allowable deflection of cranes bridge

Kind of crane	Allowable value
a) Hook crane	$\frac{1}{1000} \leq \frac{f}{L} < \frac{1}{800}$
b) Grab crane	$\frac{1}{1200} \leq \frac{f}{L} < \frac{1}{1000}$

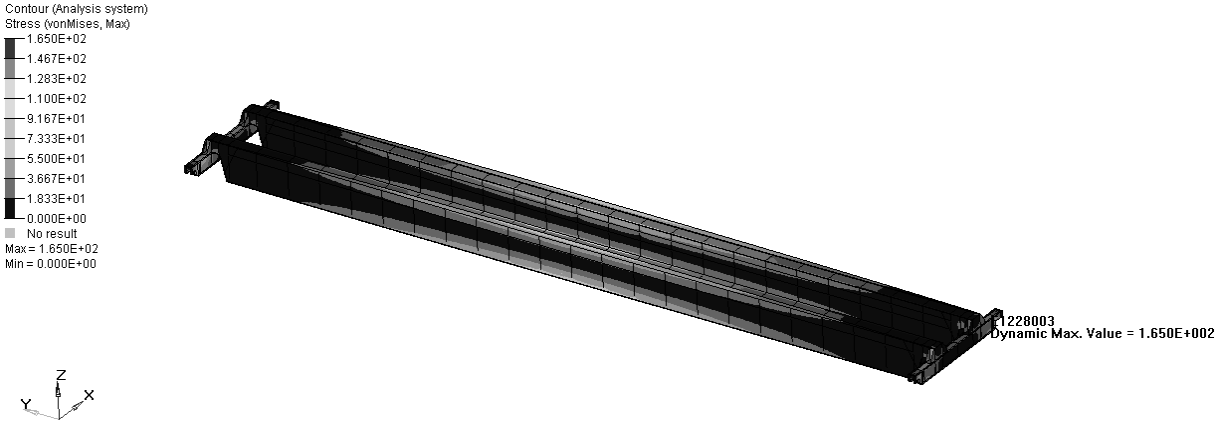

Fig. 18. Von Mises stress due to nominal load and own mass (gravity effect)
Rys. 18. Naprężenia wywołane masą ładunku oraz grawitacją

For the presentation in figures 19 and 20 are shown displacements and stresses values for the extreme left position the trolley, without taking gravity into account.

Within the study a modal analysis was performed, which allowed the appointment of the first four natural frequencies and their forms.

The calculation results for modal analysis, in turn:

- 1st form – frequency value – 2,353 [Hz];
- 2nd form – frequency value – 2,586 [Hz];
- 3rd form – frequency value – 4,261 [Hz];
- 4th form – frequency value – 4,432 [Hz].

In figures 21 to 24 the calculated structure figures for the first four natural frequencies are shown.

2.7.6. Analysis of results: displacements and form of vibrations

By using the finite element method it can be carried out several research, that in the majority are almost impossible to determine in an analytical example, i.e. modal analysis for which in the classical method it is needed to make a series of measurements. The above example also shows that this method is not very complicated and already with little effort, it can perform interesting research. It should however be taken into account that these researches can only be preliminary test, to compare actual (real) conditions with the simulation ones. This can improve the algorithm of the calculations to reflect as closely as possible the given reality. This will help in future testing the model only as a simulation using the FEM. In effect, FEM allows for cost savings during the design process.

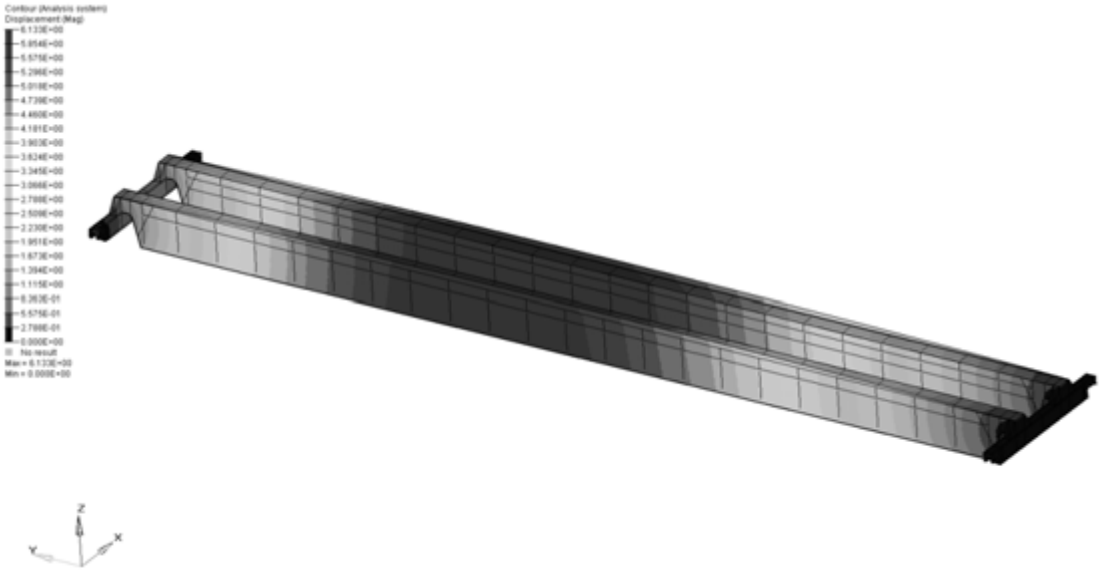

Fig. 19. Displacement for structure with nominal load 200 kN without gravity effect (trolley at left side)
Rys. 19. Przemieszczenia dla ustroju obciążonego siłą 200 kN bez uwzględnienia grawitacji (położenie lewe)

Fig. 20. Von Mises stress for structure with nominal load 200 kN without gravity effect (trolley at left side)
Rys. 20. Naprężenia zredukowane dla ustroju obciążonego siłą 200 kN bez uwzględnienia grawitacji (położenie lewe)

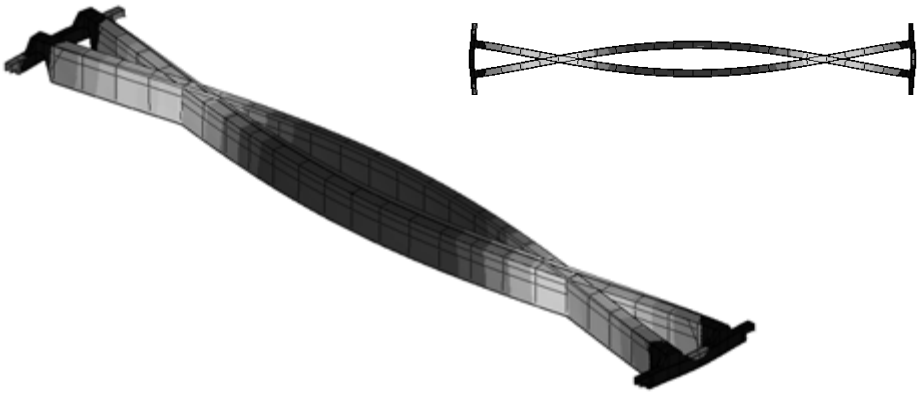

Fig. 21. Form of the first natural frequency f = 2,353 Hz of crane load-carrying structure
Rys. 21. Postać drgań ustroju pod wpływem 1. wartości częstotliwości własnej 2,353 Hz

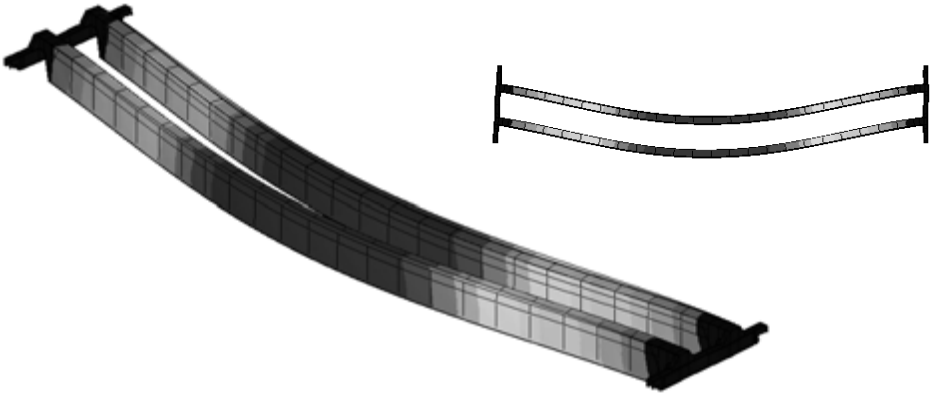

Fig. 22. Form of the second natural frequency f = 2,586 [Hz] of crane load-carrying structure
Rys. 22. Postać drgań ustroju pod wpływem 2. wartości częstotliwości własnej 2,586 Hz

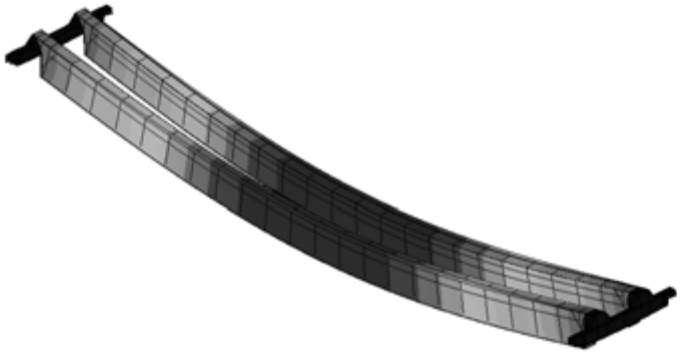

Fig. 23. Form of the third natural frequency f = 4,261 [Hz] of crane load-carrying structure
Rys. 23. Postać drgań ustroju pod wpływem 3. wartości częstotliwości własnej 4,261 Hz

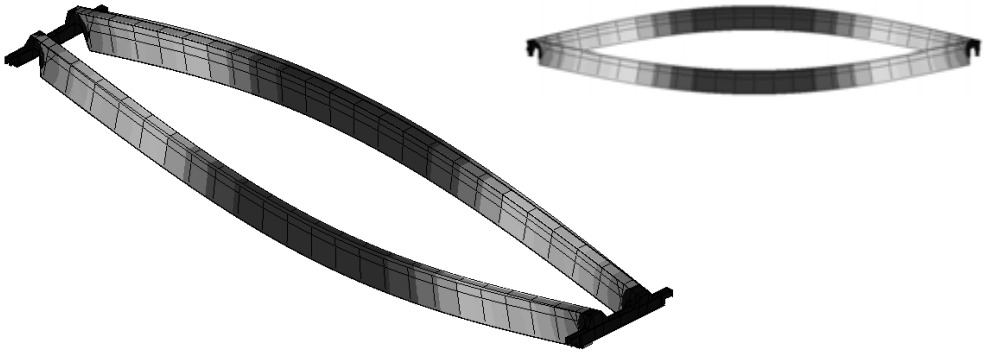

Fig. 24. Form of the fourth natural frequency f = 4,432 [Hz] of crane load-carrying structure
Rys. 24. Postać drgań ustroju pod wpływem 4. wartości częstotliwości własnej 4,432 Hz

3. FEM RESEARCH OF NEW LOAD-CARRYING CONSTRUCTION OF BELT CONVEYOR

Conveyor belts are so simple in structure and design features that provide them with considerable versatility, and in some cases resulting in that they are an indispensable means of transport, create the largest in terms of demand and production, group of transportation equipment often used in production plants for the continuous transport of bulk materials. To

optimize the technical solutions of conveyor belts (load-carrying structures), a concept of building a new type of conveyor routes repetitive element come into being. Implementation of such a solution should help to reduce operating costs and improve reliability of belt conveyors. A characteristic feature of a new type of repetitive element (fig. 25) is its innovative design with obliquely beams welded support frame in the shape of "V" letter [10].

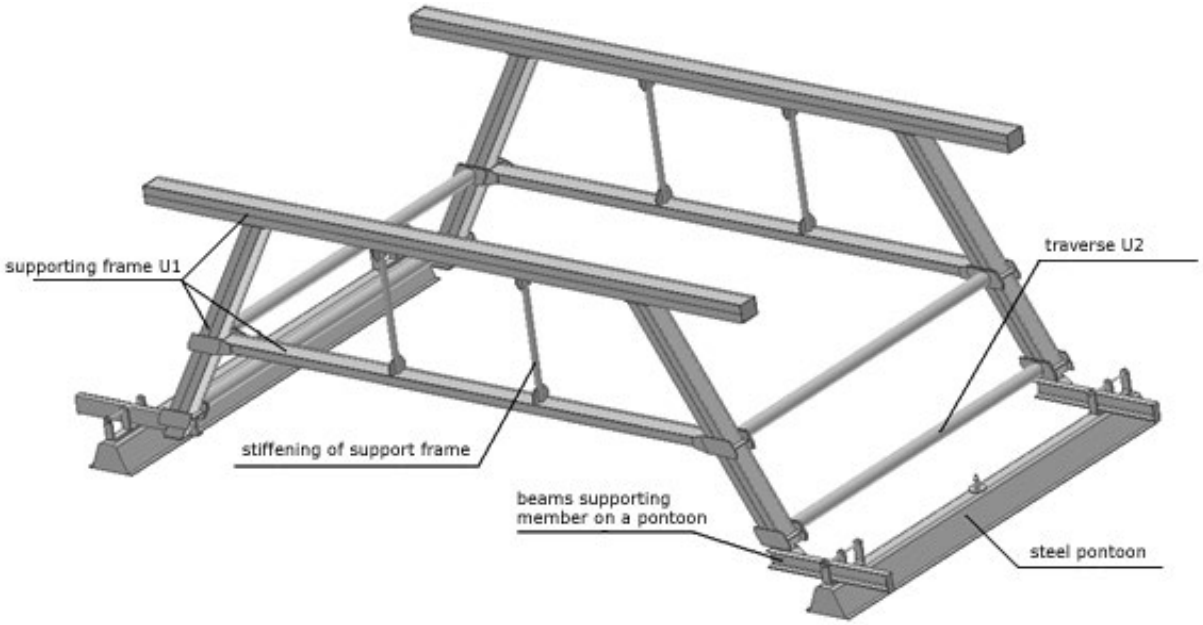

Fig. 25. Geometrical model of repetitive element „V"
Rys. 25. Model geometryczny członu powtarzalnego typu „V"

The major advantages of a new type of repetitive elements are:

- the possibility to combine them into a more stable structure (fig. 26)
- support members on the common, steel or reinforced pontoons and their connection with the pivotally mounted switches enabling turning of the conveyor by 7,5° from its axis,
- construction of a low susceptibility to subsidence as a result of loose and wet soil,
- the use of almost two times smaller number of pontoons according to traditional construction.

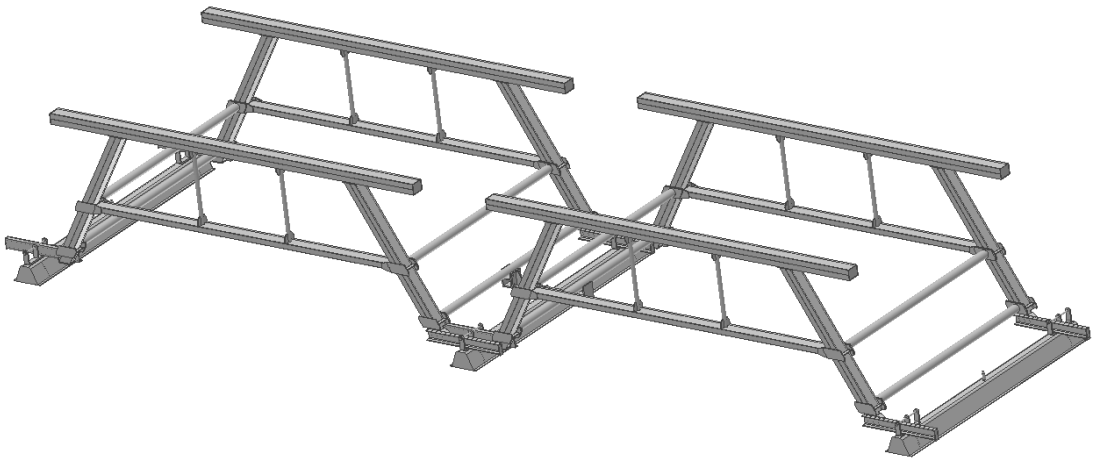

Fig. 26. Joint of two repetitive elements „V"
Rys. 26. Połączenie dwóch członów powtarzalnych typu „V"

On the load-carrying structure of repetitive element are acting forces caused by static load weight of transported material and the structure, belt, rollers. In addition, to the design of the element are acting, negligible in the calculation of static strength, dynamic loads from rotating rollers. Static loads caused by own mass of elements structure, rollers and belt are acting continues, loads due to the bulk material is variable and depends on the degree of belt loading. To determine the maximum forces acting on the element, it was assumed to be meaningful the nominal and symmetrical filling belt with material at the entire length of the member, with the symmetrical belt laying at the roller. In addition, the forces taken into account are also the burden from pollution, rainfall and wind.

Characteristic load values acting on the structure are usually static loads, so testing the strength of the repetitive elements structure was based on static analysis. The analysis of the static load-carrying structure, at a specified shape and dimensions, subjected to external loads (load constant), was based on the calculation of the stress field, displacement and deformation across its area. Implementation of stress analysis was made possible through the use of MSC.Nastran as a solver. MSC.Patran was used as the pre- and post-processor.

The repetitive elements construction model is built as a frame construction made from standard economic channel sections C160 (alternatively, rectangular shapes and dimensions 160x120x8), channel sections C120 and pipes ϕ51 i ϕ102. Load-carrying structure consists essentially of two structural frames and four crossbeams merging them using bolts. The analyzed section of solid model construction is divided into a finite number of tetrahedral elements with 10 nodes. FEM model was built from 203879 elements and 408314 nods (fig. 27). Forces were applied at nodes, in places of roller hooks. The load-carrying structure (FEM model) was supported at the contact surfaces of horizontal channel beams with pontoon construction.

For the most faithful representation of actual conditions, nodal points of one with the planes taken away all six degrees of freedom, the other were eliminated two degrees of freedom, thereby allowing the horizontal displacements in the z direction. The scheme of loads and supports is shown in fig. 28.

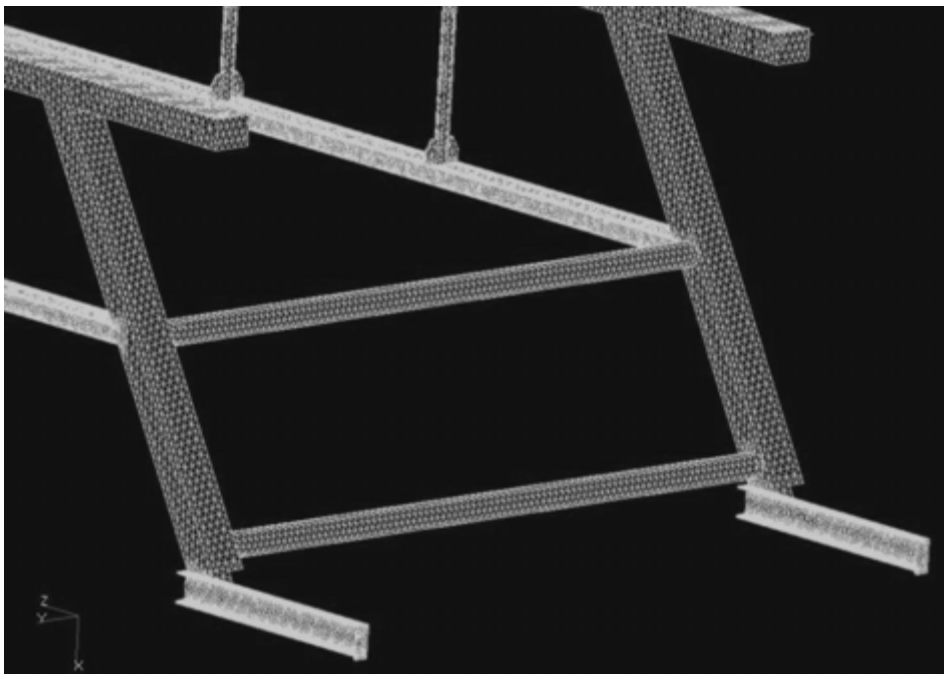

Fig. 27. Fragment of repetitive element „V-type” FEM model
Rys. 27. Fragment modelu dyskretnego konstrukcji nośnej członu powtarzalnego typu „V”

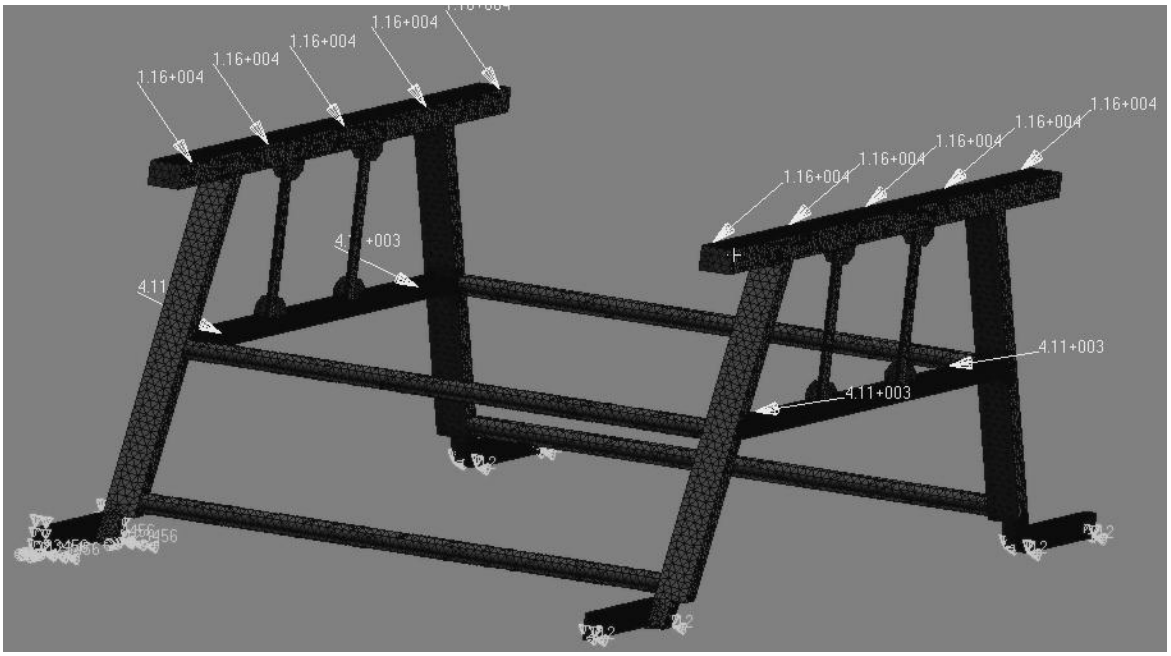

Fig. 28. Boundary conditions of repetitive element „V-type" FEM model
Rys. 28. Schemat obciążenia modelu konstrukcji nośnej wykorzystanej w analizie statycznej

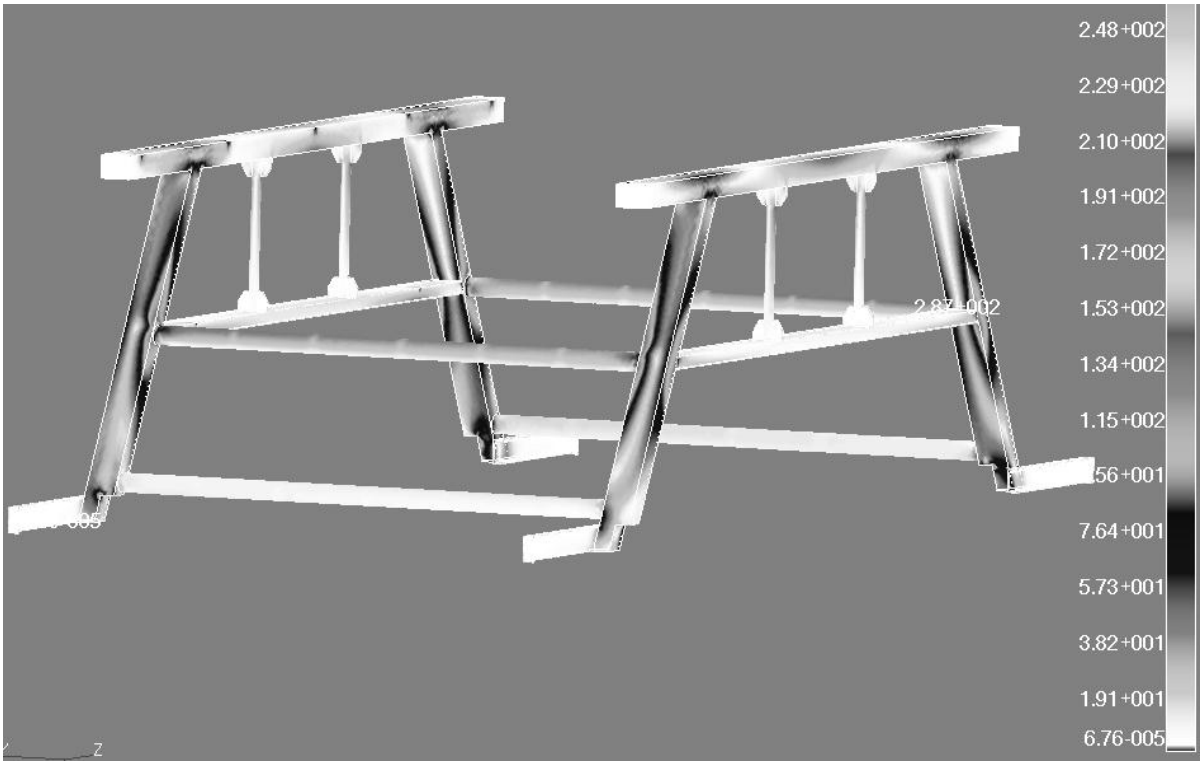

Fig. 29. Von Mises stress in repetitive element „V-type" FEM model
Rys. 29. Rozkład naprężeń w członie powtarzalnym wg hipotezy Hubera-Misesa-Hencky'ego

In a result of the analysis a stress distribution according to Huber-Mises-Hencky (von Mises stress) hypothesis is shown in fig. 29. Maximal value of stress σ_{max}=287 [MPa] is located in joint place of construction frame U1 with cross beams U2 (fig. 30). In these joints the strengthen of the load-carrying structure should be placed.

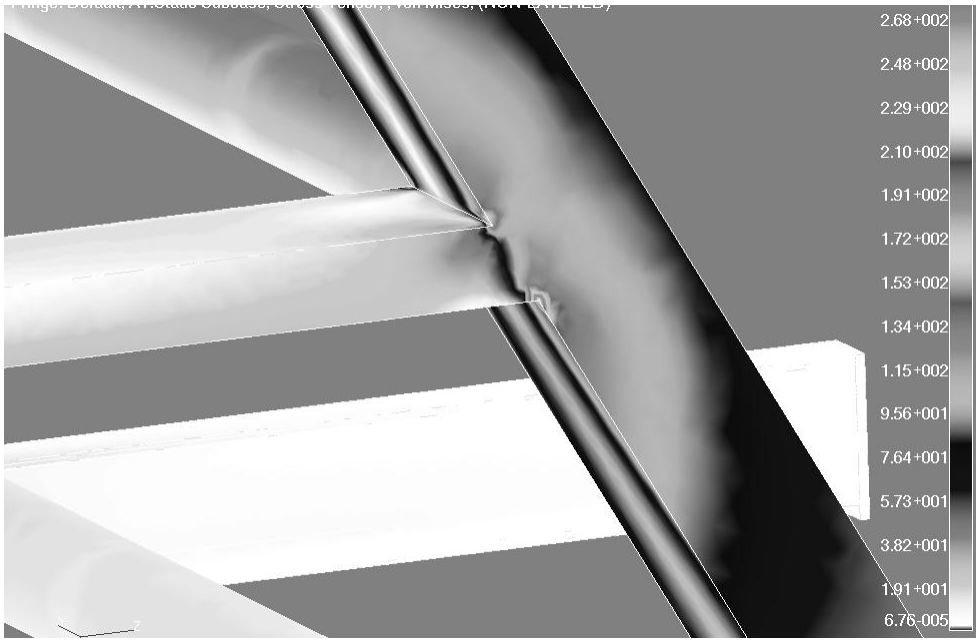

Fig. 30. Local maximal stress value at the joint place of construction frame U1 with cross beams U2
Rys. 30. Lokalne spiętrzenie naprężeń w członie powtarzalnym na połączeniu ramy nośnej z poprzecznicą

An important result of strength analysis is also a map of the displacements of the load-carrying structure (fig. 31). The maximum displacement value f_{max} is approximately 7.5 [mm]. As expected, the largest displacements are occurring in the horizontal beams, towards the axis of symmetry of the beam.

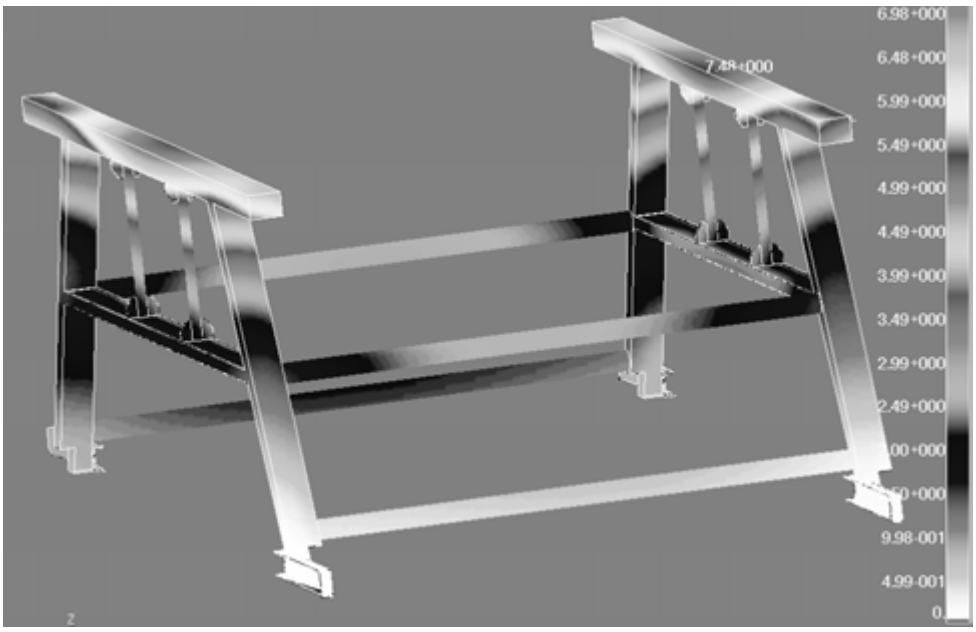

Fig. 31. Displacements in repetitive element „V-type" FEM model
Rys. 31. Rozkład przemieszczeń w modelu konstrukcji nośnej członu powtarzalnego

The results of the repetitive element „V-type" strength show that the design assumptions are correct in terms of durability, the greatest use of strength, however reaches 93%. A small surplus is to ensure the safety of welded contacts for alternative loads that were not subject of the calculation.

4. CALCULATION OF ELEVATORS RACK LOCK IN OVERHEAD CONVEYOR ON THE PRODUCTION LINE OF CAR FACTORY

Transport systems are one of the most important elements of the car assembly lines. Right properties of the chosen transport system are most important in case of line efficiency as well as safety. One of the devices performing functions of handling is a lift, installed on the production line of Fiat Panda (fig. 32). The unloading from the overhead conveyor onto the floor conveyor is performed on it. Lift consists of the load-carrying structure - two columns connected by transverse beams, after which the rack moves [11].

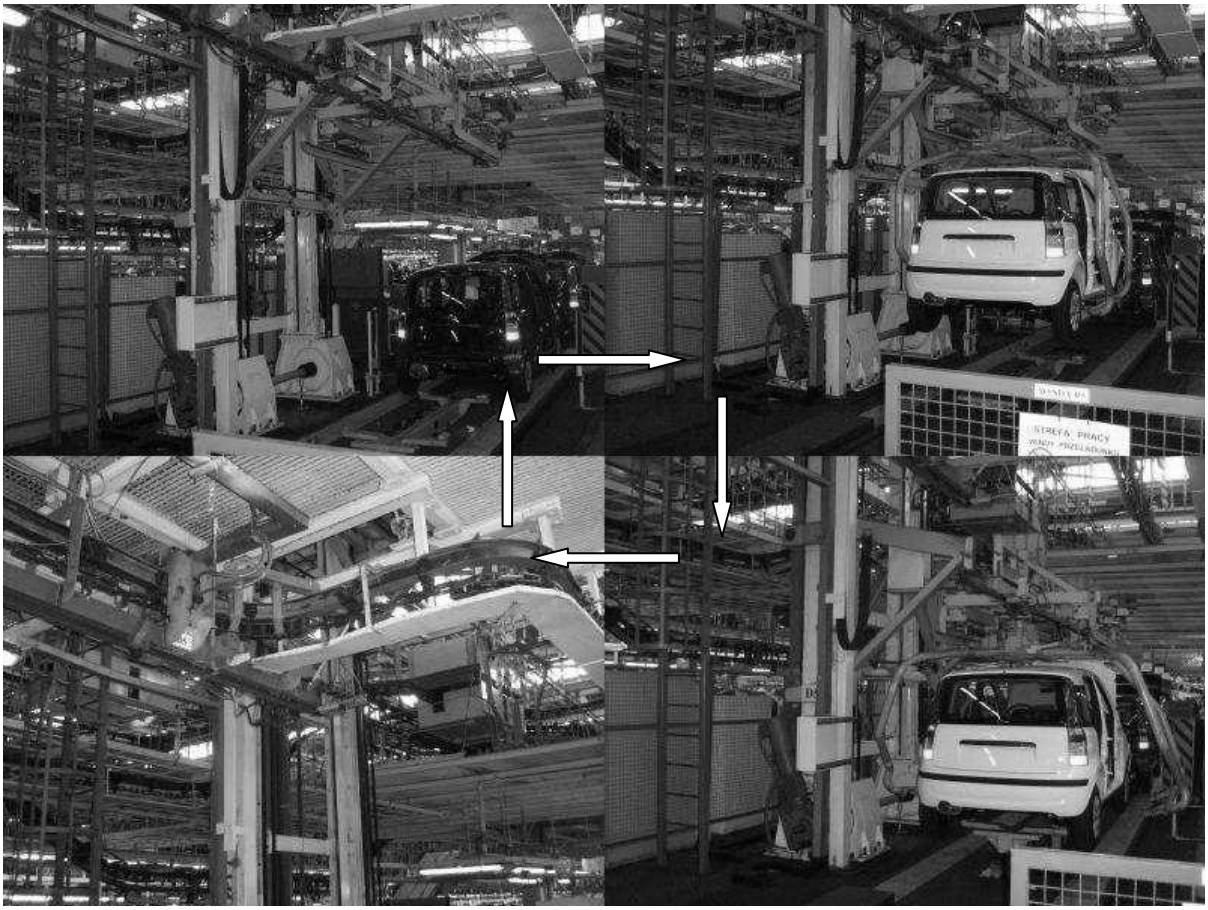

Fig. 32. Lift duty cycle
Rys. 32. Cykl pracy windy

At the time when the rack with the body, entry of the overhead conveyor to lift, the rack is being left a few mm, and then returns to normal position. Because in case of the strength of materials such acting phenomenon is not good (may occur fatigue), the task of lock is mechanically lock the hanger and do not allow to change position.

Lock was designed in a way to ease the implementation and maintenance. It consists of a small number of elements, so that its safety factor increases (fig. 33).

Elevators rack lock consists of elements:

- racks (left 4 and right 5 bars in fig. 33) - two movable parts of lock, moving relative to each other in the horizontal direction, their move aside provide a point of resistance for the rack;
- fasteners - these are elements with which the rack lock is attached to the load-carrying structure of the lift. Mounts (1, 2) are attached to the lift columns, while the holder 3 is based on the structure attached to a crossbeam;

- mechanism of motion - the mechanism consists of a gear wheel 6 cooperating with the two profiled racks 4 and 5 (fig. 33c).

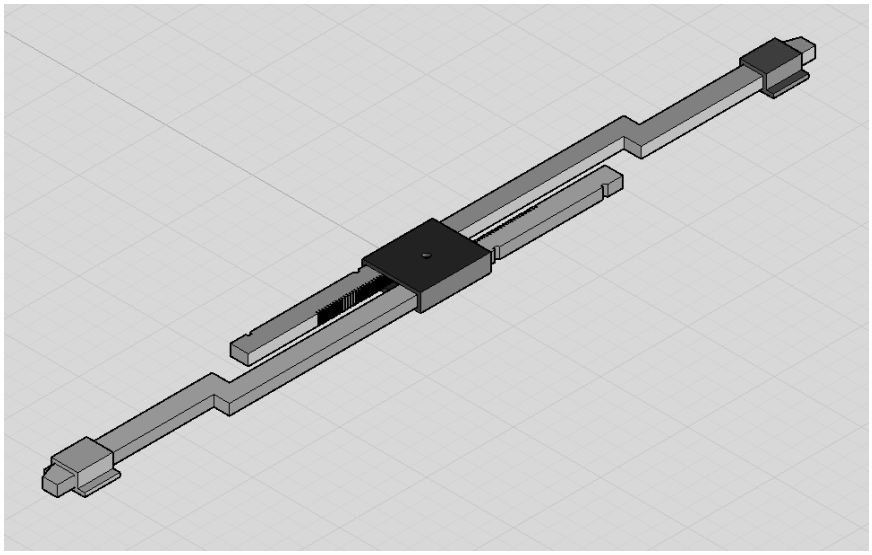

a

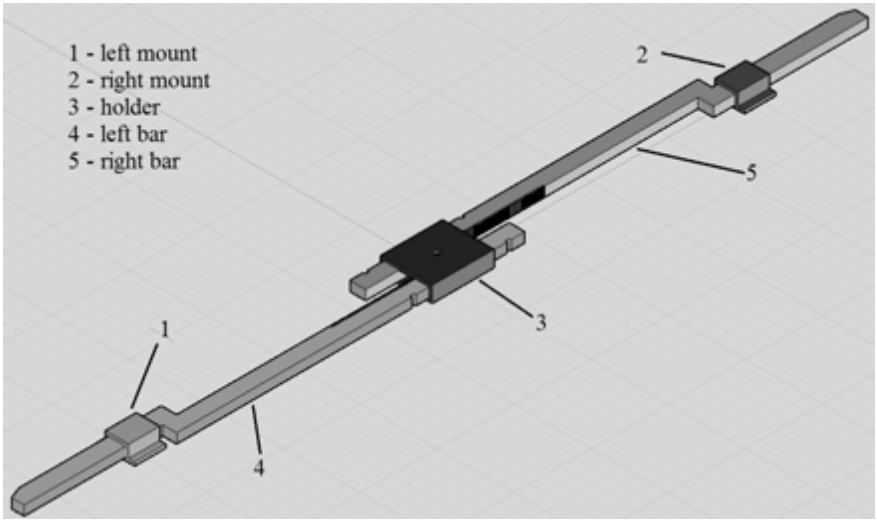

b

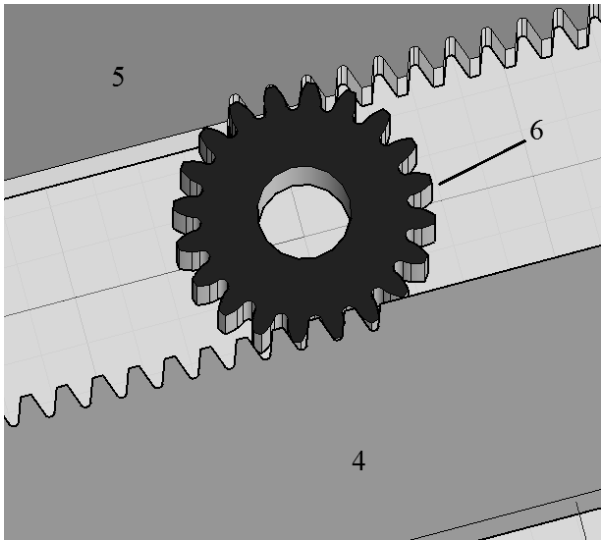

c

Fig. 33. Elevators rack lock: a – state open; b – blocked state; c – toothed wheel cooperating with the two profiled toothed bars

Rys. 33. Blokada windy wieszaka: a – stan otwarty; b – stan zablokowany; c – koło zębate współpracujące z zębatkami rygli

In the strength calculation MSC.Marc software as a solver was used (due to the necessity of resolving the issue of contact) but as a pre-and post-processor MSC.Patran. The whole model was divided into 6-nodes and 8-nodes spatial elements [12]. In some cases, certain simplifications are made, for example, reduced the number of examined teeth for gear wheel and racks (fig. 34), it is clear in comparison with fig. 33c.

For a proper strength analysis it was necessary to determine the appropriate boundary conditions (fig. 35), which consists of the anchoring (indicated by arrows), and the forces acting on the elements of the lock. Must also set contact bodies. All loads are the forces that were adopted under the racks force of gravity which was based on the beams. An extreme situation was analysed – when body is on a rack, and the force resulting from the weight of the rack is not limited by no additional protection and with the body amounts by Q = 18000 [N].

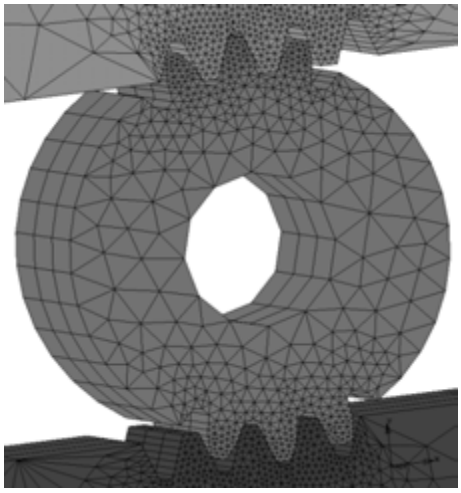

Fig. 34. Simplifications of the mesh for gear wheel and racks
Rys. 34. Uproszczenia siatki dla modelu koła zębatego współpracującego z zębatkami rygli

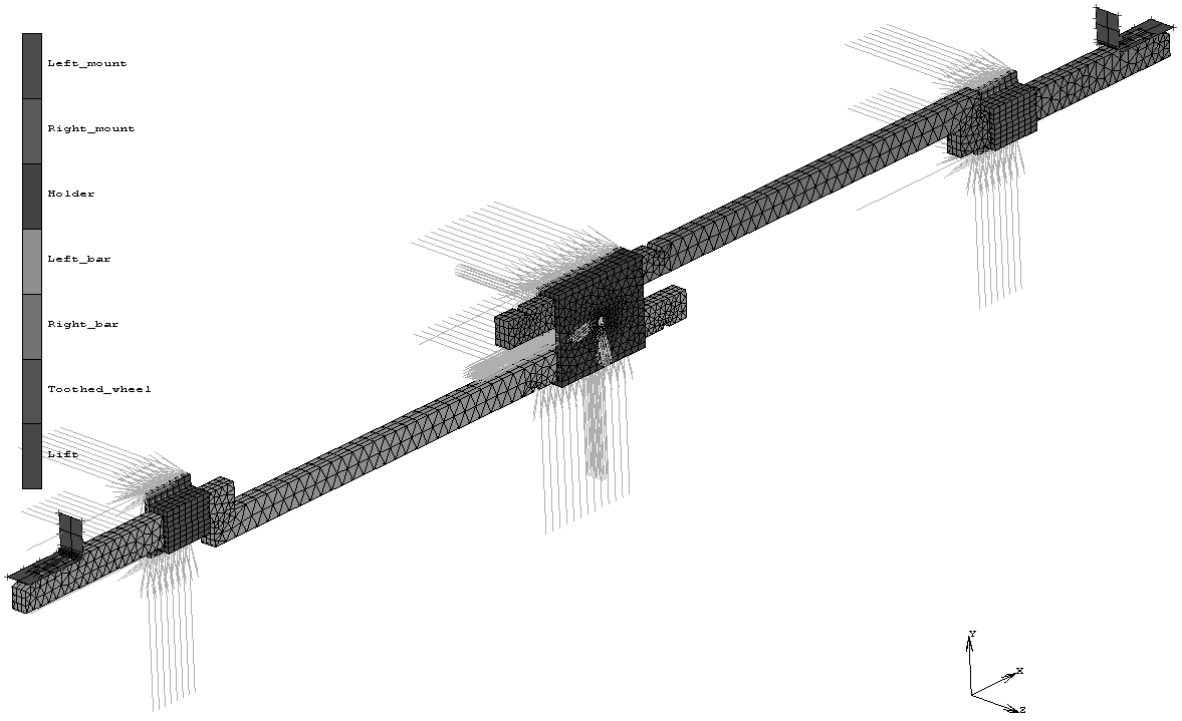

Fig. 35. Setting of contact bodies and boundary conditions for the model of elevators rack lock
Rys. 35. Model blokady z podziałem na ciała kontaktowe

As expected the greatest stress in elevators rack lock occurred at the place of support for racks (fig. 36). The maximum stress value is relatively small and reaches 156 [MPa], it operates on a very small volume of the rack and poses no threat to the safe operation of the lock.

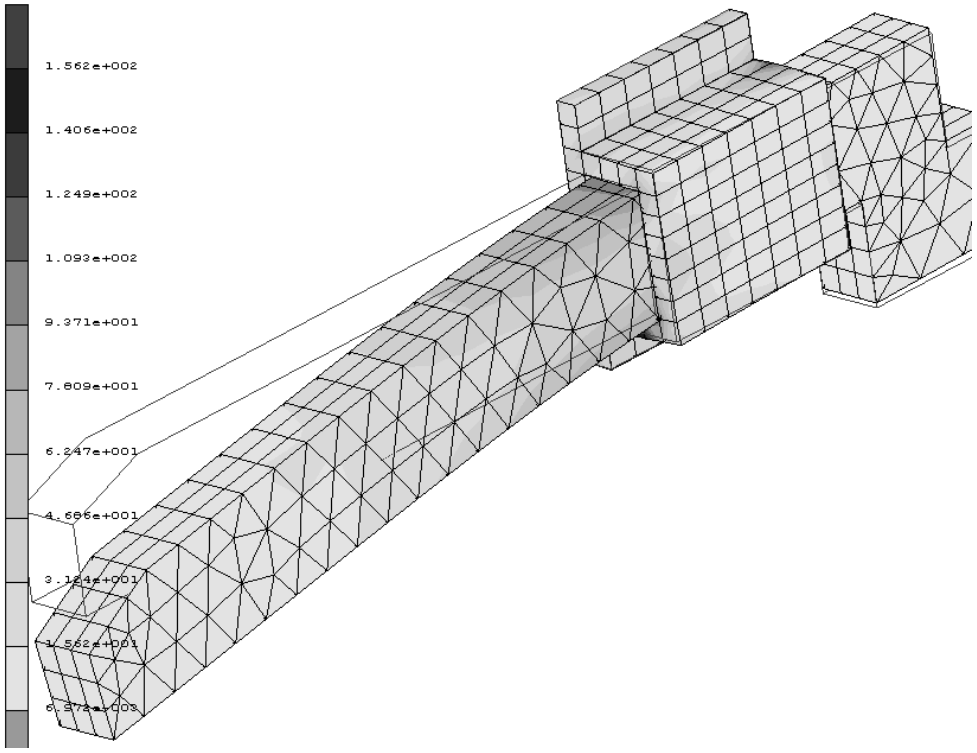

Fig. 36. Von Mises stress in elevators rack lock (mounting area, displacements are increased by 50 times)
Rys. 36. Rozkład naprężeń w ryglu wg hipotezy Hubera-Misesa-Hencky'ego

Another area with high levels of stress is gearing. The stress distribution in this area is shown in fig. 37.

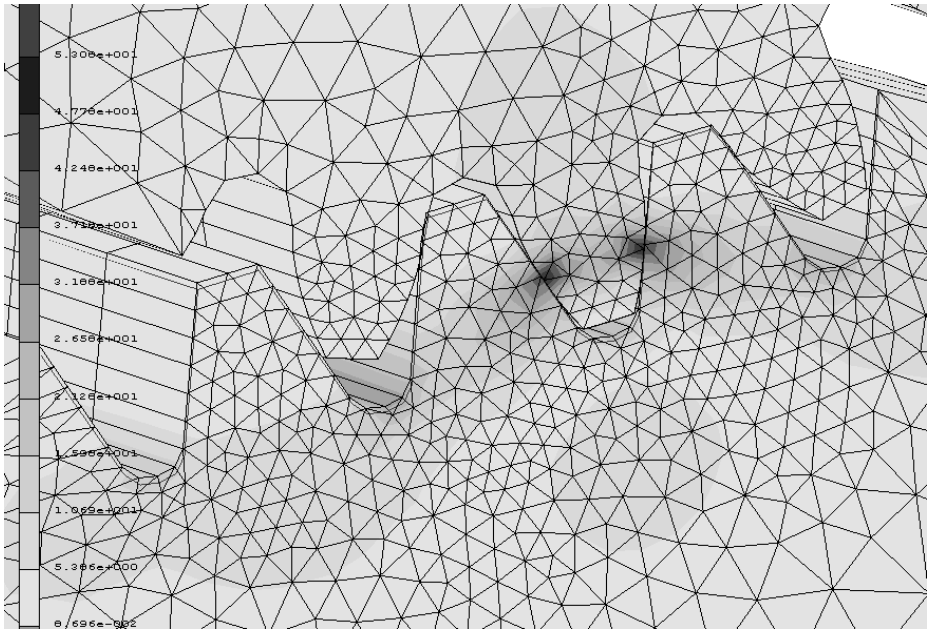

Fig. 37. Von Mises stress in the gearing area
Rys. 37. Model rozkładu naprężeń koła zębatego współpracującego z zębatkami

The maximum stress level 53 [MPa] for this area is achieved in the contact between the gear wheel and the lower (left) gear rack. The value obtained is several times less than the maximum stress that occurred in this construction. Safety factor for such a construction must have a high value.

5. STRENGTH CALCULATIONS FOR A SPECIAL TECHNOLOGICAL PALLET

Passive means of transport such as pallets are used in various industrial plants [13]. The most popular are the standard europallets, however, the technological process often requires the use of special pallets (fig. 38). One of the examples of such pallet can be a special one used to storing and transport of various components (fig. 39). The analyzed palette was used in the process of picking specific structural elements in the production of car upholstery (fig. 39) [14].

Fig. 38. Special technological pallet
Rys. 38. Paleta technologiczna

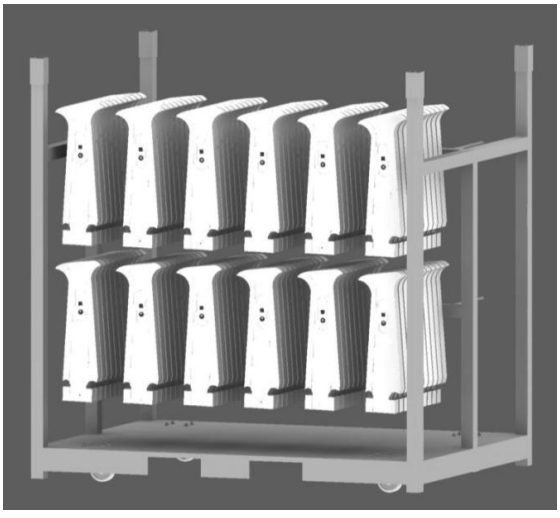

Fig. 39. Special technological pallet with specific structural elements in the production of car upholstery
Rys. 39. Paleta technologiczna wraz z elementami konstrukcyjnymi

In the strength calculations of pallet loaded with structural elements the MSC.Nastran as a solver and MSC.Patran as pre- and postprocessor were used. The model was divided into tetra elements.

For a proper analysis of the strength it was necessary to determine the appropriate boundary conditions (fig. 40), which consists of the attachment, and the forces acting on the smooth bars.

Palette is based on the ground by the wheel sets, or will get in contact with another unit load during storage. For the case of the analysis second case was chosen, all nodes located on the lower surfaces of steel profile were restrained.

On each smooth bar will hold 10 special structural components, each weighing 1.5 kg. Therefore, for the FEM analysis it was assumed that for each bar works 10 forces with the value of 15 [N]. These forces have been restrained in the spot nodes, in the site of contact with the surface of the bar element, and with proper distance (fig. 40).

As expected the greatest stress on the bars occurred in close proximity to attachment to steel profile. Stress value (fig. 41) oscillates in the range 34-130 [MPa]. The maximum stress is not a threat to the safety of construction. The place where the bars are fixed is characterized by reaching the maximum stress limit of 60 [MPa]. This is also relatively low value which in no way affects the possibility of breaking under the weight of the hanging elements.

Displacements are also low, and at the end of the bar amounts 2 mm. As for the thin elongated element it is a relatively small value. Thanks to the cutouts in the bar under the suspended elements, there will be no slipping of the detailing, even if the deviation were larger. The analysis showed that the structure is designed to hang heavier items which can be used in future.

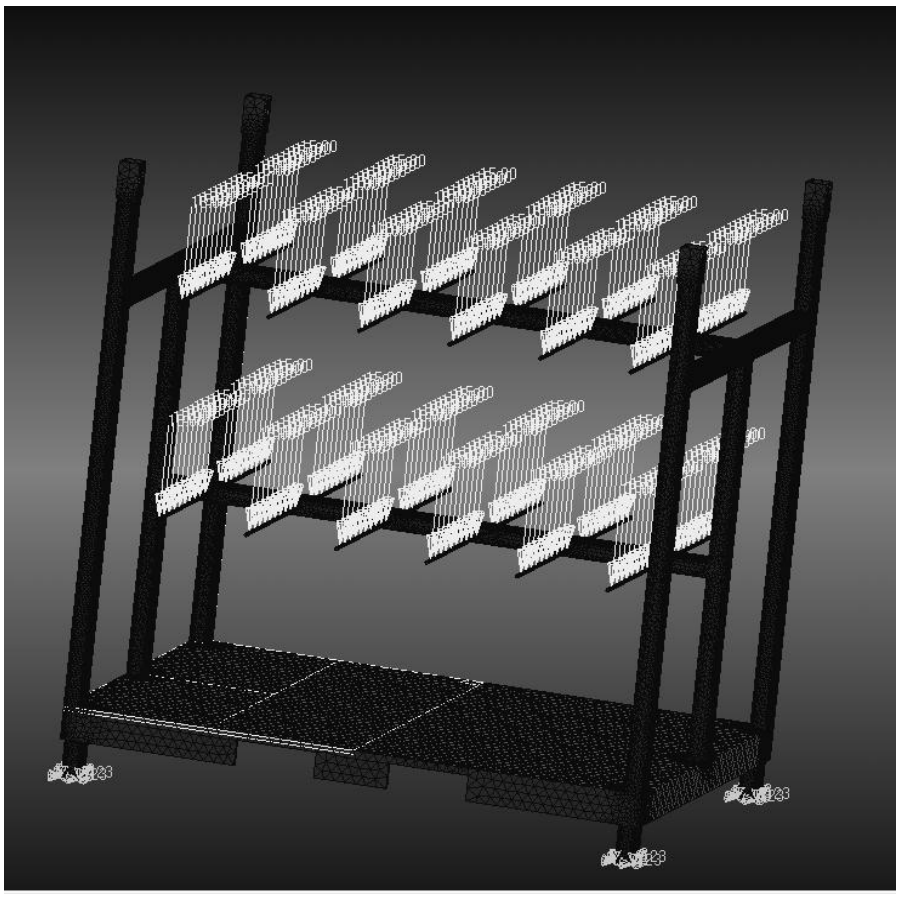

Fig. 40. FEM model with boundary conditions
Rys. 40. Model palety z zaznaczeniem warunków brzegowych

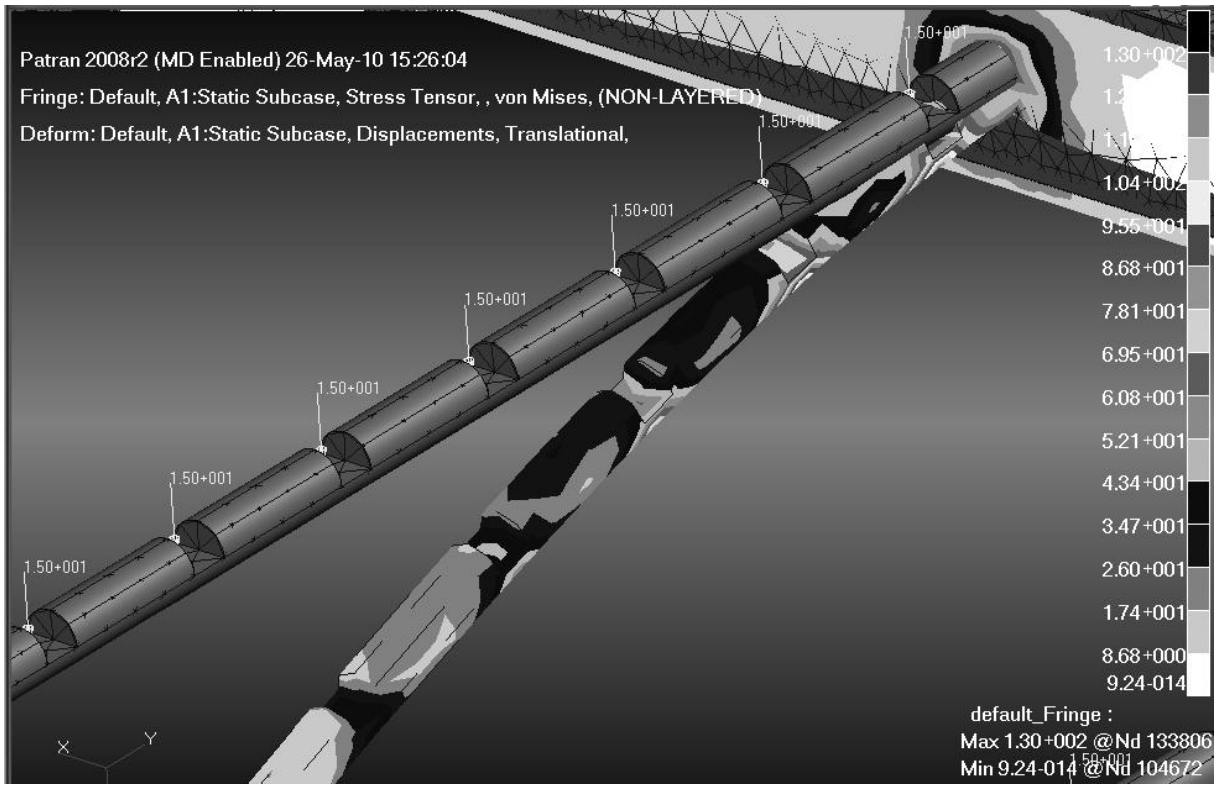

Fig. 41. Von Mises stress in bar
Rys. 41. Rozkład naprężeń zredukowanych

6. STRENGTH CALCULATIONS OF BRIDGE CRANE GIRDERS

In the process of manufacturing, raw materials, semi-finished and finished products are moved in different directions, both – within the industrial plant and outside it, and the basic means of transport used in this process are the cranes. The basic cranes include overhead and bridge cranes. Evolution of their load-carrying structures is mainly based on reducing cost and time to produce them with their strength remained unchanged or even improved [15]. Obtaining such a result is possible thanks to new technology and methods of computation (e.g. finite element method).

The load-carrying structure of bridge cranes is made in the shape of a one- or double-girder bridge. Gantries load-carrying structures with large span and large capacity, are constructed as a box-section double-girder. On the girders are installed rails, which make street of the trolley. To the girders are mounted platforms with railings. Girders are supported on four supports placed on beams in which the wheels are installed [16].

Bridge crane that undergone durability calculations (fig. 42, fig. 43) is a double-girder-type U structure with supports from which the so-called pivot support is fastened to the hinge in the plane of the gate, while the second is called constant support, is fixed rigidly to the girders. Construction load-carrying crane structure consists of metal sheets and is a typical shell structure. Discretization of this model using shell elements is most effective because of the computing capabilities of the computer and the accuracy of the results.

Fig. 42. Bridge crane under consideration
Rys. 42. Przykład suwnicy kontenerowej poddanej obliczeniom wytrzymałościowym

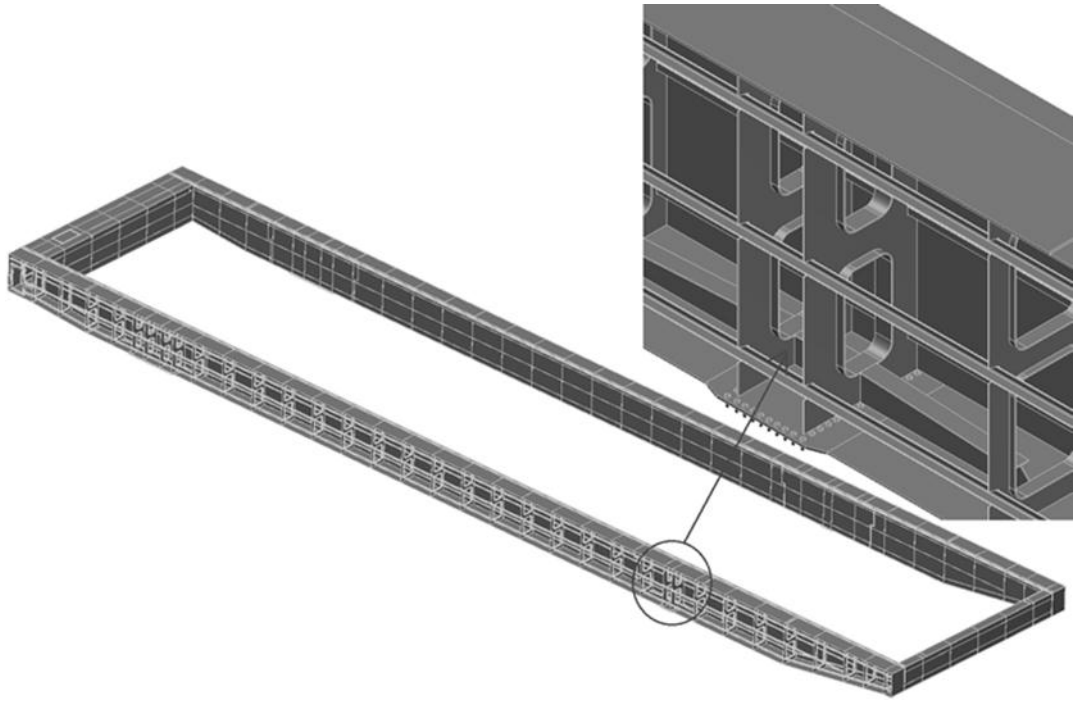

Fig. 43. Geometrical model of girders structure
Rys. 43. Model geometryczny dźwigarów ustroju nośnego suwnicy

In order to use solid elements to shell model, while maintaining the appropriate proportions relative lengths of sides and a minimum number of elements in the thickness of the sheet metal, it could be that such a task would be very difficult or impossible to solve.

Due to the fact that the crane load-carrying structure is a typical shell structure to divide the elements CTRIA3, CQUAD4, CHEXA, RBE2, CBAR from MSC.Nastran library of finite elements were used. The MSC.Patran as a preprocessor was used. Forces coming out from proper loads combinations were simulated as concentrated (acting on node) or as pressure (wind forces) and acceleration (gravity). The models were supported in support planes. On one side of the crane all degrees of freedom were blocked, while on the other side (pivot support) the X-axis displacement and rotation in Z-axis were not.

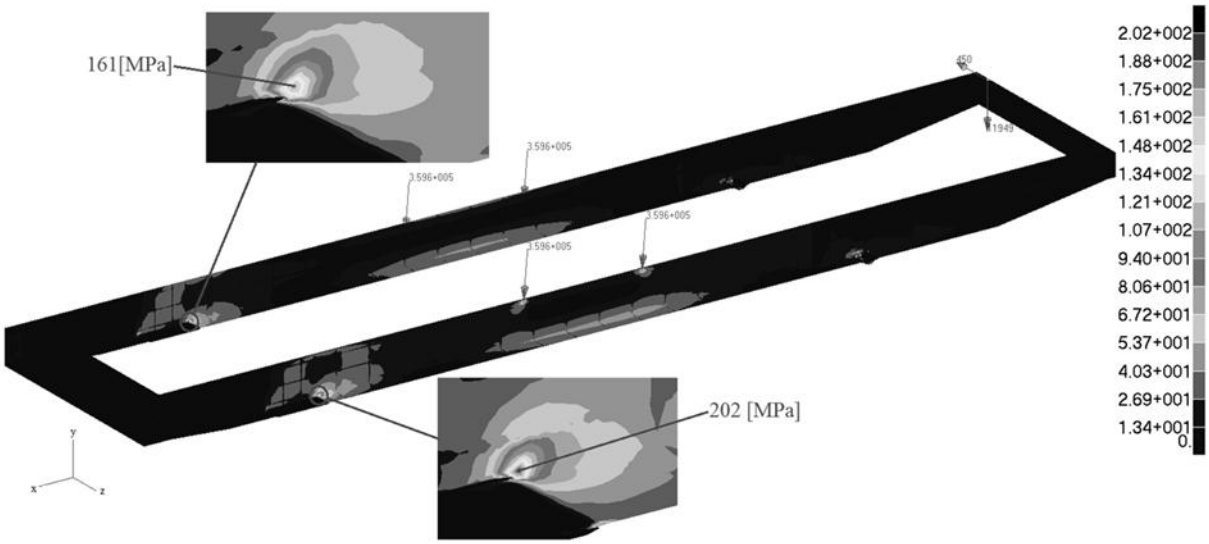

Fig. 44. Von Mises stress values for load-carrying crane structure at B1 load combinations according to [19]. Winch in the middle of the crane span

Rys. 44. Rozkład i zakres naprężeń zredukowanych dla kombinacji obciążeń B1 (zgodnie z [19]) ustroju nośnego mostu suwnicy bramowej, wciągarka w środku rozpiętości

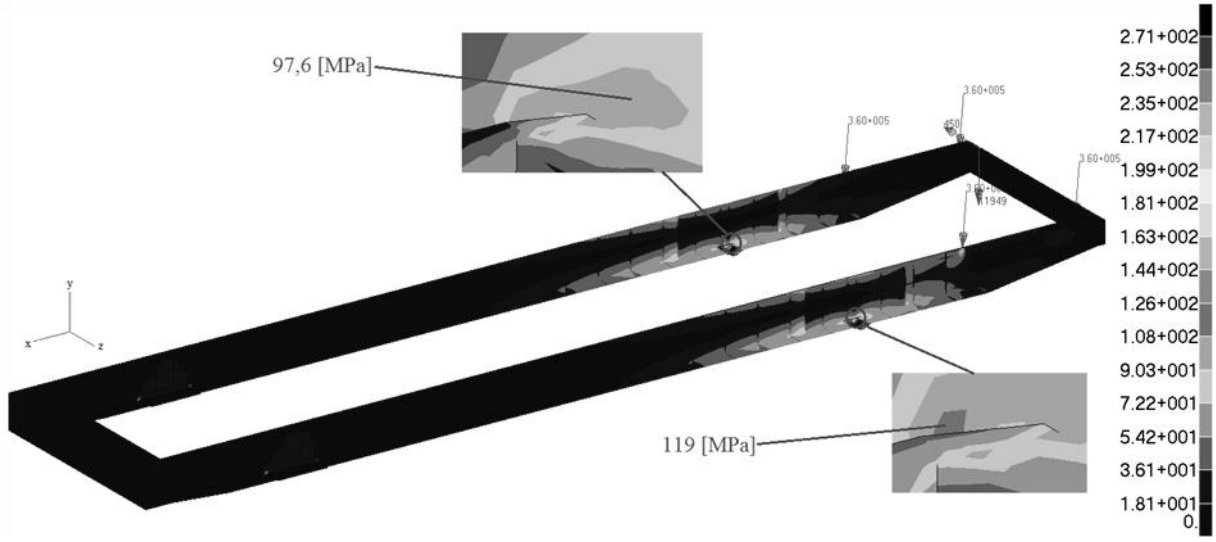

Fig. 45. Von Mises stress values for load-carrying crane structure at B1 load combinations according to [19]. Winch behind the pivot support

Rys. 45. Rozkład i zakres naprężeń zredukowanych dla kombinacji obciążeń B1 (zgodnie z [19]) ustroju nośnego mostu suwnicy bramowej. Wciągarka za podporą wahliwą

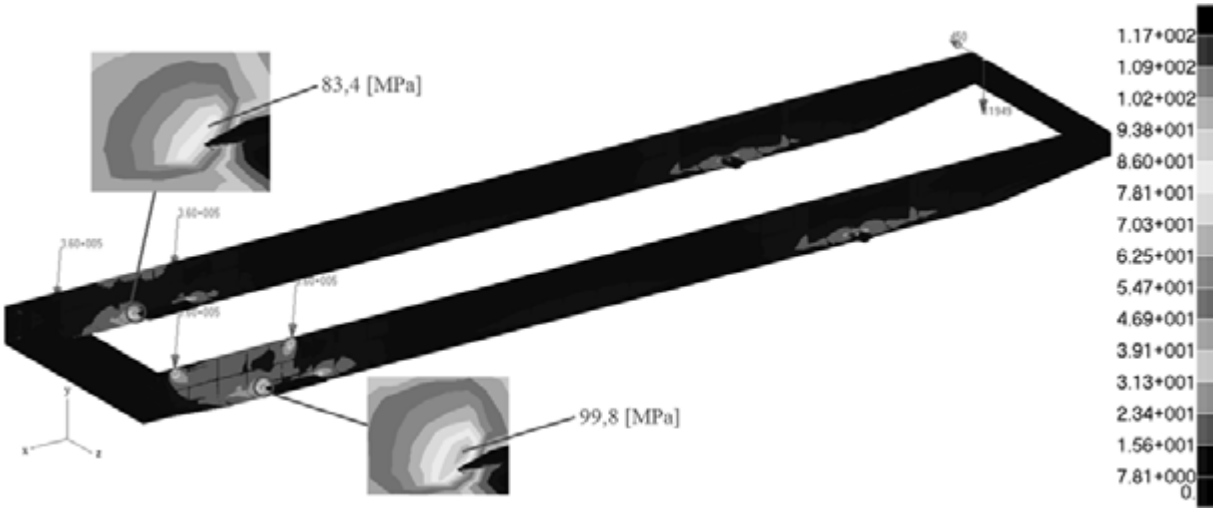

Fig. 46. Von Mises stress values for load-carrying crane structure at B1 load combinations according to [19]. Winch behind the constant support

Rys. 46. Rozkład i zakres naprężeń zredukowanych dla kombinacji obciążeń B1 (zgodnie z [19]) ustroju nośnego mostu suwnicy bramowej. Wciągarka za podporą stałą

7. MODELING INFLUENCE OF SIMPLIFICATIONS ON STRESS AND STRAIN STATE IN 450 T CRANES HOISTING WINCH CONSTRUCTION

We can observe the development of international technical standardization, assume that the development in the domain of calculations [23, 24, 29] and manufacture eliminate some dangers generated in the past (70s, 80s and 90s when most of cranes being used now were designed). In this study the FEM analysis of stress and strain state of the selected trolley's load-carrying structure with 450 tones hoisting capacity was made. This analysis could be an introduction for cranes load carrying structures and drives calculations already made [25, 26, 27] and for those which will be made in future.

Model of trolley was built from several cooperating with each other (in contact) parts. Main parts of hoisting winch load – carrying structure (fig.47) being under consideration are:

- 450 t pulley block girder (1) – free laying on buffer beams (5),
- 80 t pulley block girder (2) – free laying on buffer beams (5),
- 4 rockers,
- 2 buffer beams (5) together with connection beams.

Fig. 47 shows also the slide limiter (4)

FEM model of the winch was built in three parts:

- frame bearer (headstocks with connected beams, with rockers, but without the rail cars which are omitted in the model);
- 450 t pulley block girder;
- 80 t pulley block girder.

Preliminary analysis of the entire system of winch, allowed to highlight a few important structural nodes:

- connections between rockers and buffer beams;
- connections between rockers and rail cars (support in axes modelled);
- slide connections between girders and buffer beams.

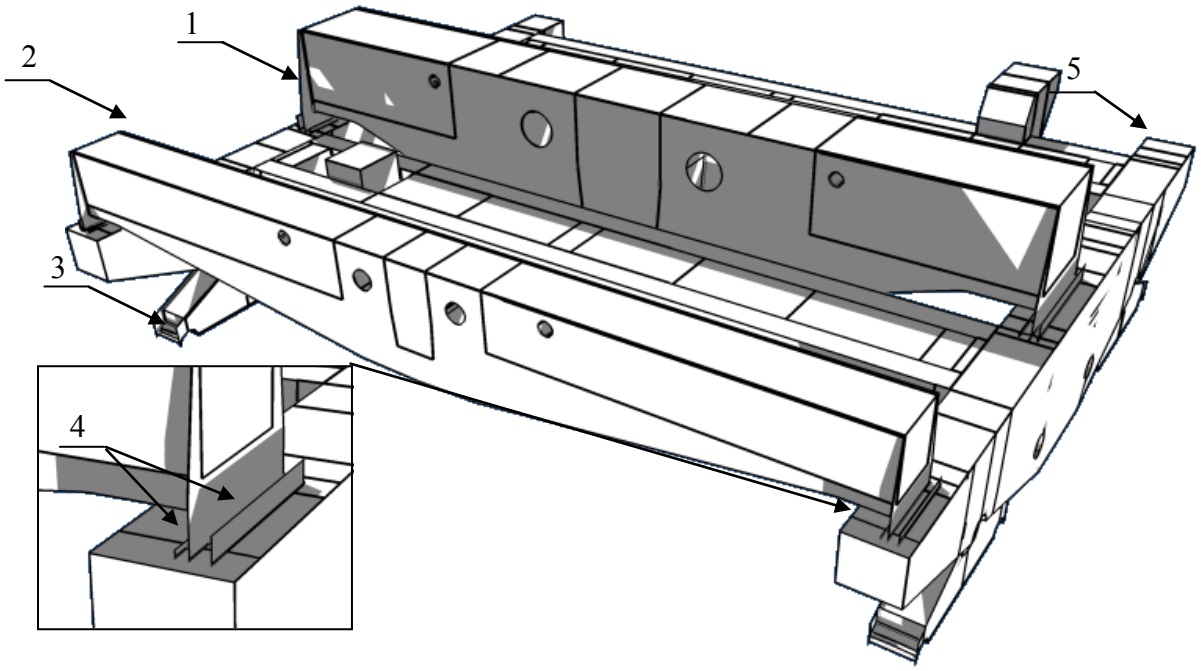

Fig. 47. Load carrying hoisting winch structure
Rys. 47. Ustrój nośny wciągarki

Three kind of models with different level of simplification – time needed for preparation and computation were considered.

Basic model (A) was made as simplified as possible and with minimal time for preparation needed. Connections between buffer beams and rockers and also girders with buffer beams were assumed as rigid (without joint rotation). The axes between rail cars and rockers wasn't being modelled. Therefore only adjoining nodes (picked directly) of rockers FEM mesh were supported. It was simplified and made faster the mesh generation which was build up only from shell elements.

In extended model (B) kinematic coupling and distributing coupling elements for axes between rockers and rail cars and also joints (connections between buffer beams and rockers) were applied.

In full model (C) also contact elements "node to surface" and "surface to surface" were applied for modeling the slide between girders and buffer beams.

The frame bearer (C and B models) was supported in axes connecting rockers and rail cars. For one axe 6 degree of freedom were taken away, and the all other only the Y and Z directions (fig. 48).

For all models loads were calculated according to standard PN-EN 13001−2:2006 [19]. Loads are shown in table 6 (fig. 48 shows the way how loads were applied).

Hoisting and gravity effects acting on the mass of the load – carrying winch structure, 450 t engine, 80 t engine, 450 t gear, 80 t gear, 450 t rope drum and 80 t rope drum were applied. All loads were multiplied by dynamic factors according to [19].

Fig. 48. Loads diagram
Rys. 48. Schemat obciążeń modelu

Table 6

The values of the forces applied to the load – carrying winch structure

Name	Value	Unit
Gravity effects acting on the mass of the load – carrying winch structure	1,48E+01	m/s^2
Gravity effects acting on the mass of 450 t engine	1,10E+04	N
Gravity effects acting on the mass of 80 t engine	1,10E+04	N
Gravity effects acting on the mass of 450 t gear	1,04E+05	N
Gravity effects acting on the mass of 80 t gear	1,93E+04	N
Hoisting and gravity effects acting on the mass of 450 t rope drum	6,57E+05	N
Hoisting and gravity effects acting on the mass of 450 t girder	5,07E+06	N
Hoisting and gravity effects acting on the mass of 80 t rope drum	1,78E+05	N
Hoisting and gravity effects acting on the mass of 80 t girder	1,06E+06	N

N, mm, MPa system of units was applied, therefore results of stresses are in MPa and displacements I mm shown. The load – carrying winch structure was made from S355 where the limit design stress for sheets thickness < 63 mm is 305 MPa [20]. The basic model (A) was made up of 69829 elements and 68200 nodes.

Calculations were made using the cluster IBM BladeCenter HS21 with Linux RedHat, 56 nodes (112 processors Intel Xeon Dual Core 2.66 GHz) and computation power 1192 Gflops. The solver was Abaqus 6.9 EF1 according to MNiSW/IBM_BC_HS21/PŚląska/021/2010 grant.

Calculations for A and B models was made in two stages (steps). In the first one gravity effects acting on the mass was applied and the hoisting effects in the second one.

For C model calculations were made similarly but in the first stage no contact was being analysed and girders (in reality free lying on the buffer beams) were hold thanks to additional boundary conditions. In second stage all other loads were applied and both girders were set free. Thanks to contact elements girders were hold on buffer beams.

As it could be done in model A, simplifications (overrigids) caused local stress concentrations. Maximal computed stress in rockers with buffer beams connections exceeded significantly the limit design stress (fig. 49). No slide possibility between girders and buffer beams caused sheets bending (fig. 50). At the other parts of the structure stresses and displacements values are similar to those from A and B models.

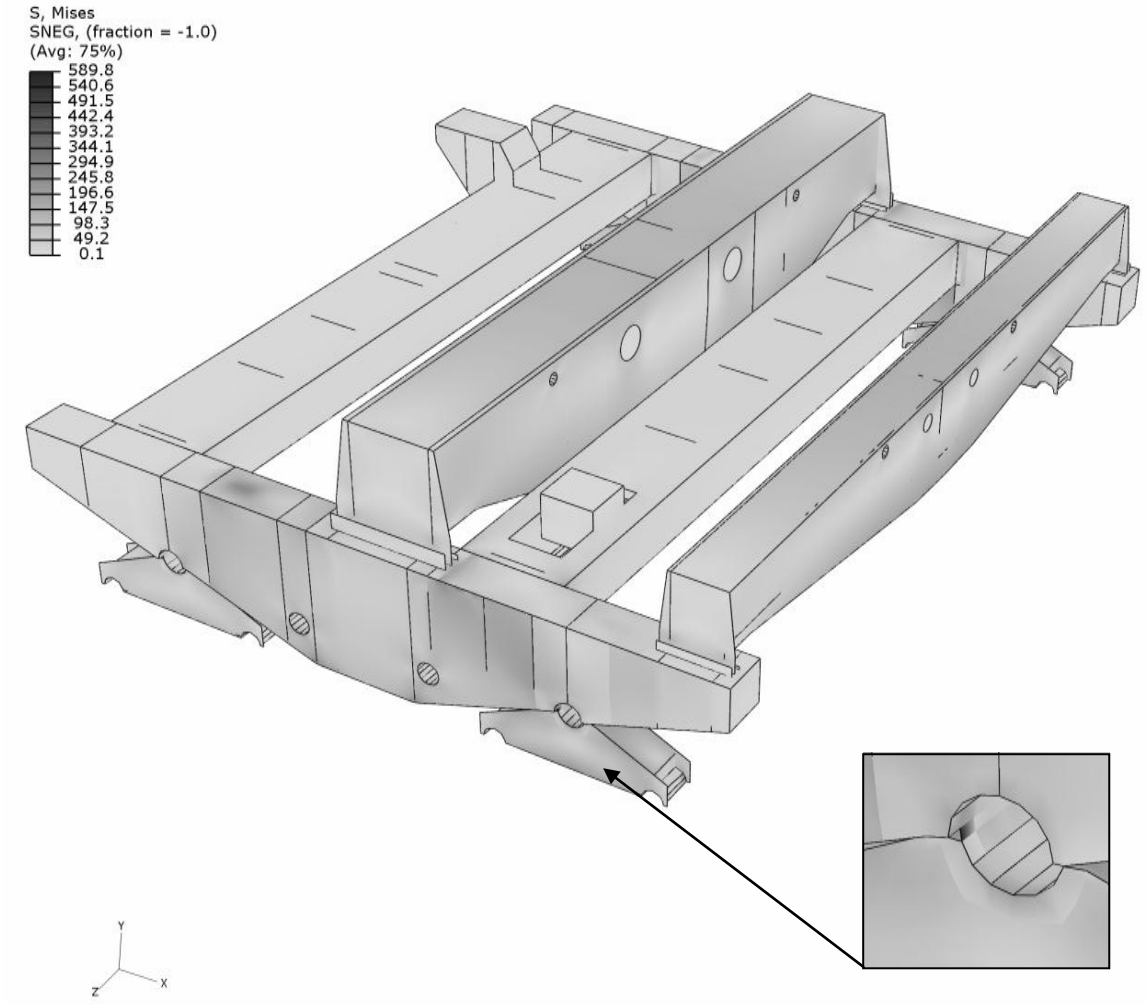

Fig. 49. Stress in the hoisting winch construction (model A) according to Huber-Mises-Hencky theory
Rys. 49. Mapa naprężeń konstrukcji (model A) wg teorii Hubera-Misesa-Hencky'ego

In model B axes connecting rockers and rail cars were modelled. Also kinematic coupling for rotation with the rockers in relation to buffer beams were applied. It was noticed that kinematic coupling was the stress concentrator in rockers axes (780 MPa – fig. 51b). Application of distributing coupling [21] generated a much better effect in these places (70 MPa – fig. 51a).

Maximal computed stress in B model decreased in relation to model A and reached 300 MPa. Stress concentration (distinguished place in fig. 52) on girder sheets connection results from no slide possibility between girder and buffer beam. Time of computation in case of model B was 3 minutes (using computer with Intel Core 2 Duo 2.5 GHz about 35 minutes).

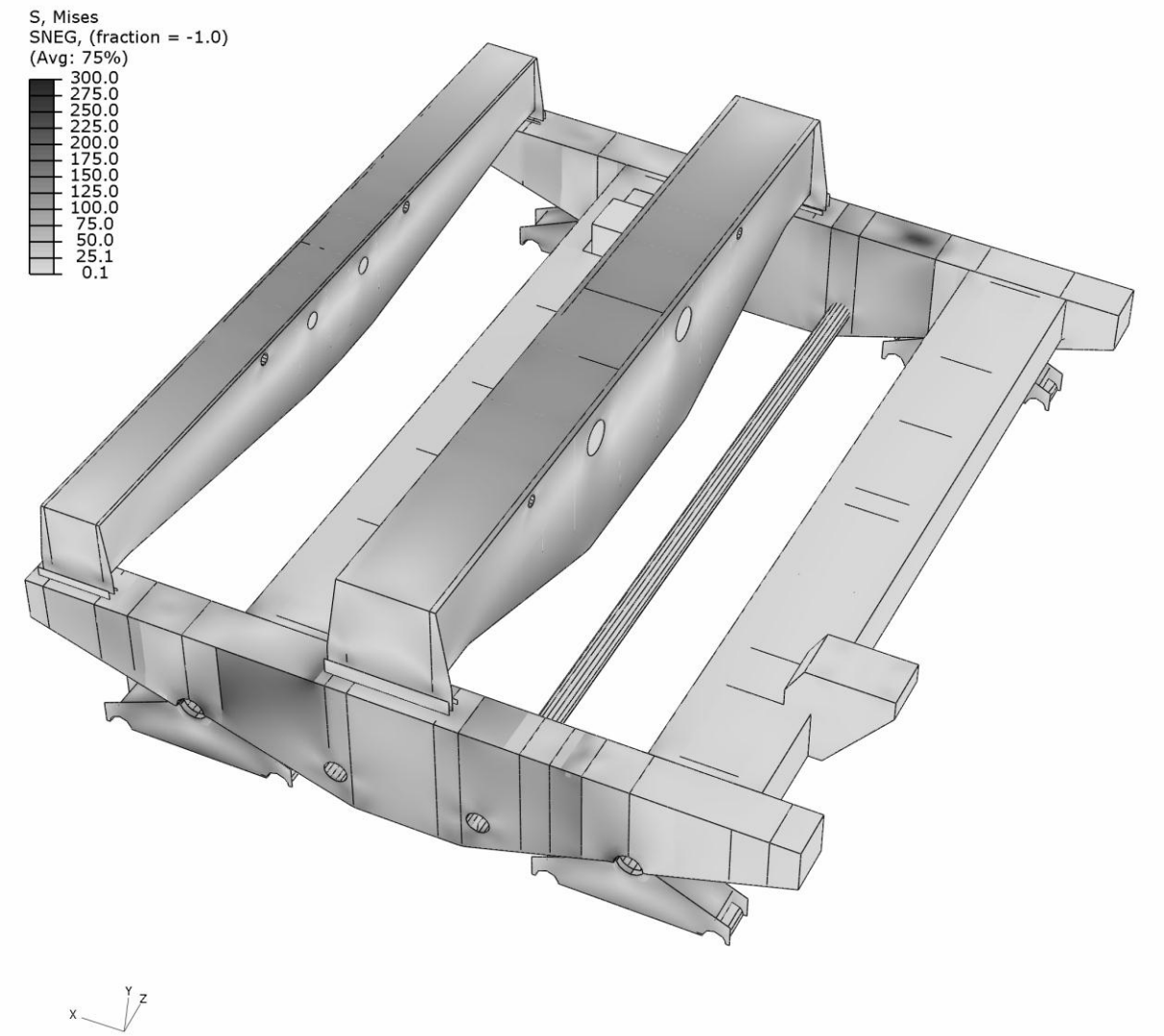

Fig. 50. Stress in the hoisting winch construction (model A) according to Huber-Mises-Hencky theory
Rys. 50. Mapa naprężeń konstrukcji (model A) wg teorii Hubera-Misesa-Hencky'ego

a) Distributing coupling b) Kinematic coupling

Fig. 51. Coupling type
Rys. 51. Typ połączenia

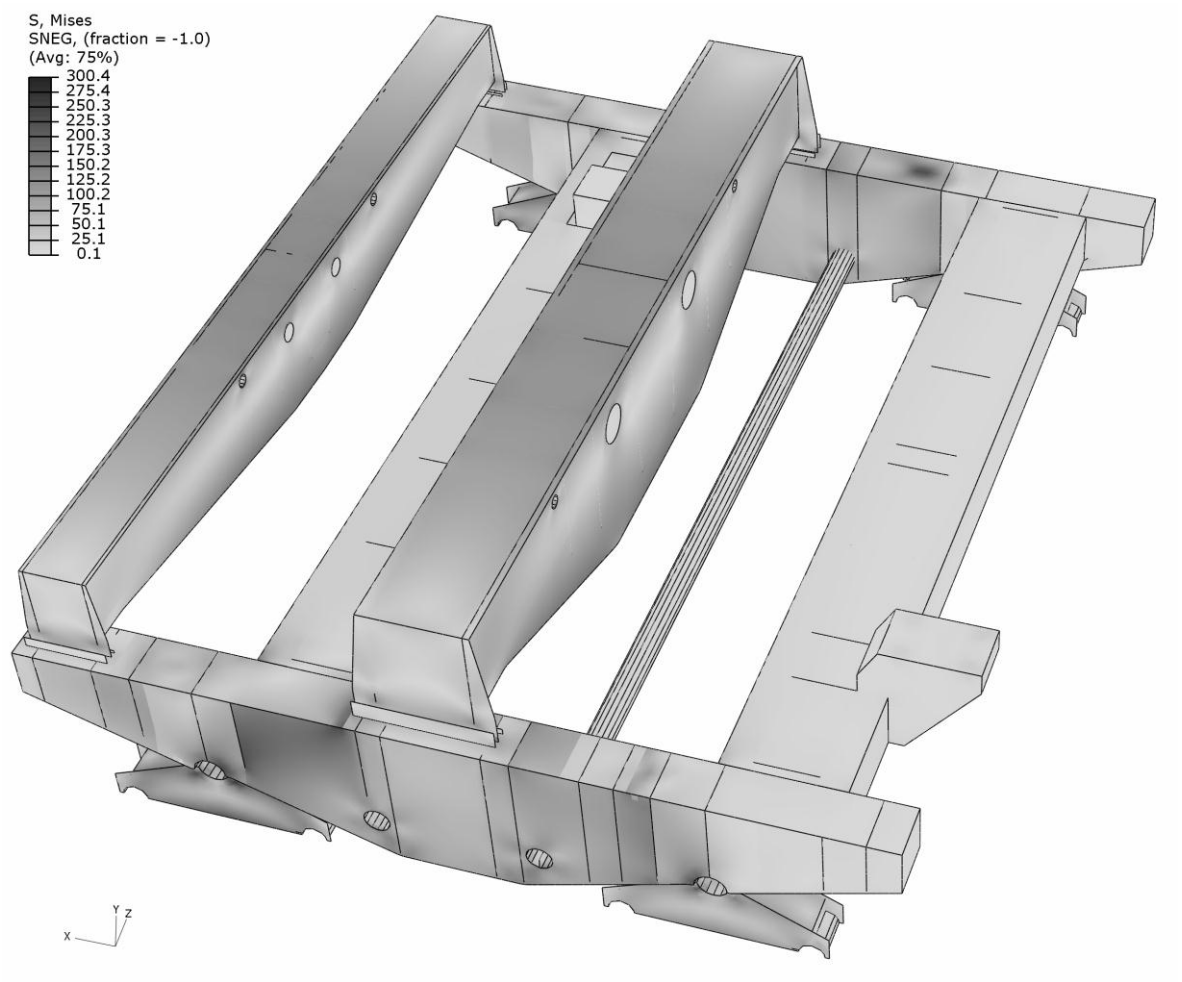

Fig. 52. Stress in the hoisting winch construction (model B) according to Huber-Mises-Hencky theory
Rys. 52. Mapa naprężeń konstrukcji (model B) wg teorii Hubera-Misesa-Hencky'ego

In model C not only the kinematic coupling but also contact elements, allowing for girders sheets slide over the buffer beams, were applied. The friction factor was assumed as 0,3. Additional contact elements "surface to surface" limit the slide size where the friction factor was assumed as 0,1. Fig. 53 shows the pressure in contact surfaces according to Huber-Mises-Hencky theory. Maximal stress in C model occurs at the edge of buffer beams bottom and are in amount of 294 MPa (fig. 54).

Fig. 55 is a diagram showing the displacement on the girders edge, sliding on the winch's buffer beam. Maximal displacement is in the range of 0,6 – 1,2 mm, by 5 mm clearance. Displacement of the whole structure shows fig. 56. There won't be any contact between supporting and limiting sheet. Therefore it is no sense of making contact in this place. Without contact in this place the computation time is three times faster. Time of computation with simplified C model was 20 minutes (using computer with Intel Core 2 Duo 2.5 GHz about 100 minutes).

The results of C model were compared with fourth alternative for contact analysis model, in which girders were modelled as two independent beams on two pivot bearing (one movable). Stress, displacement and support reactions were computed. This support reactions were treated as loads acting on buffer beams in connection with girders area. Results were almost the same as in model C and the time of computation much shorter. Friction influence between girder and buffer beam is therefore not big.

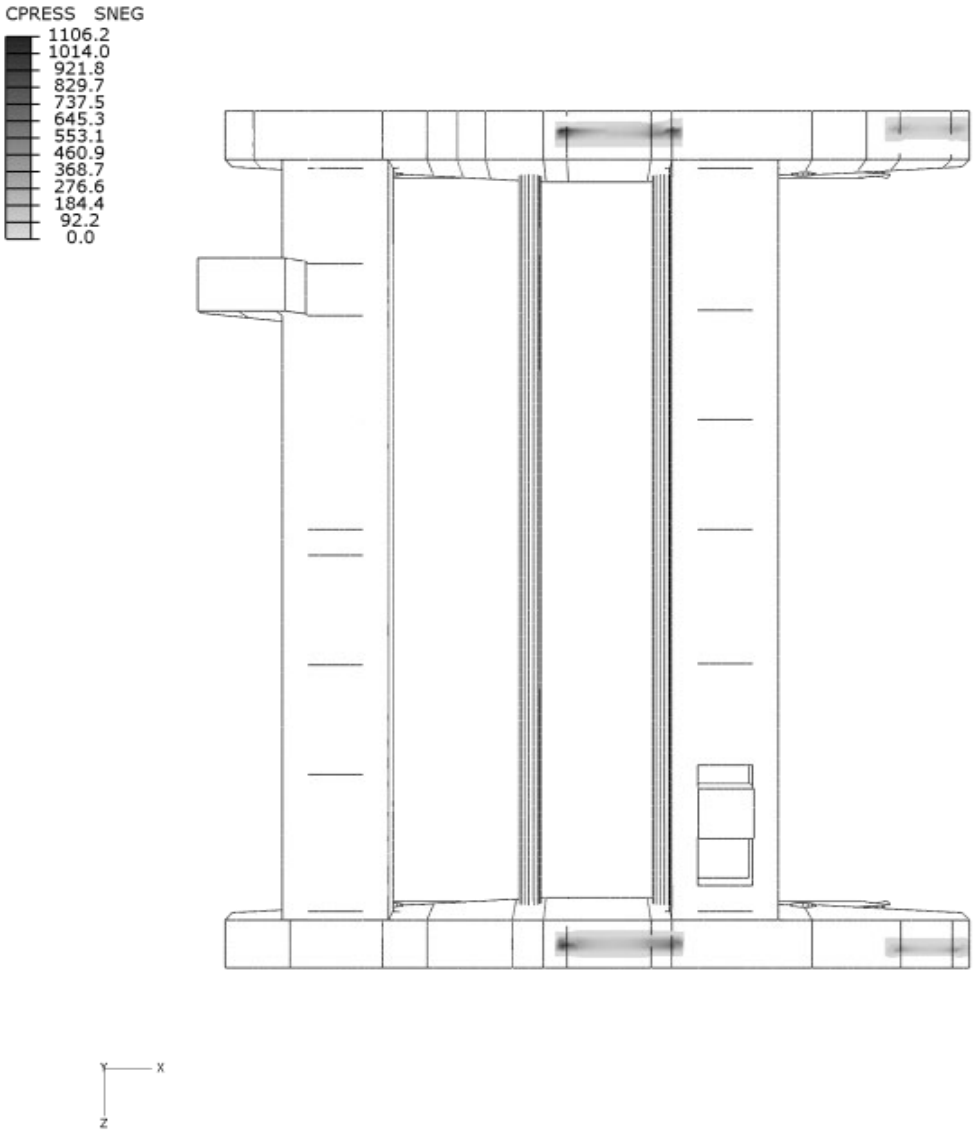

Fig. 53. Pressure in contact surfaces according to Huber-Mises-Hencky theory (model C)
Rys. 53. Mapa rozkładu ciśnienia na powierzchniach kontaktowych konstrukcji (model C)

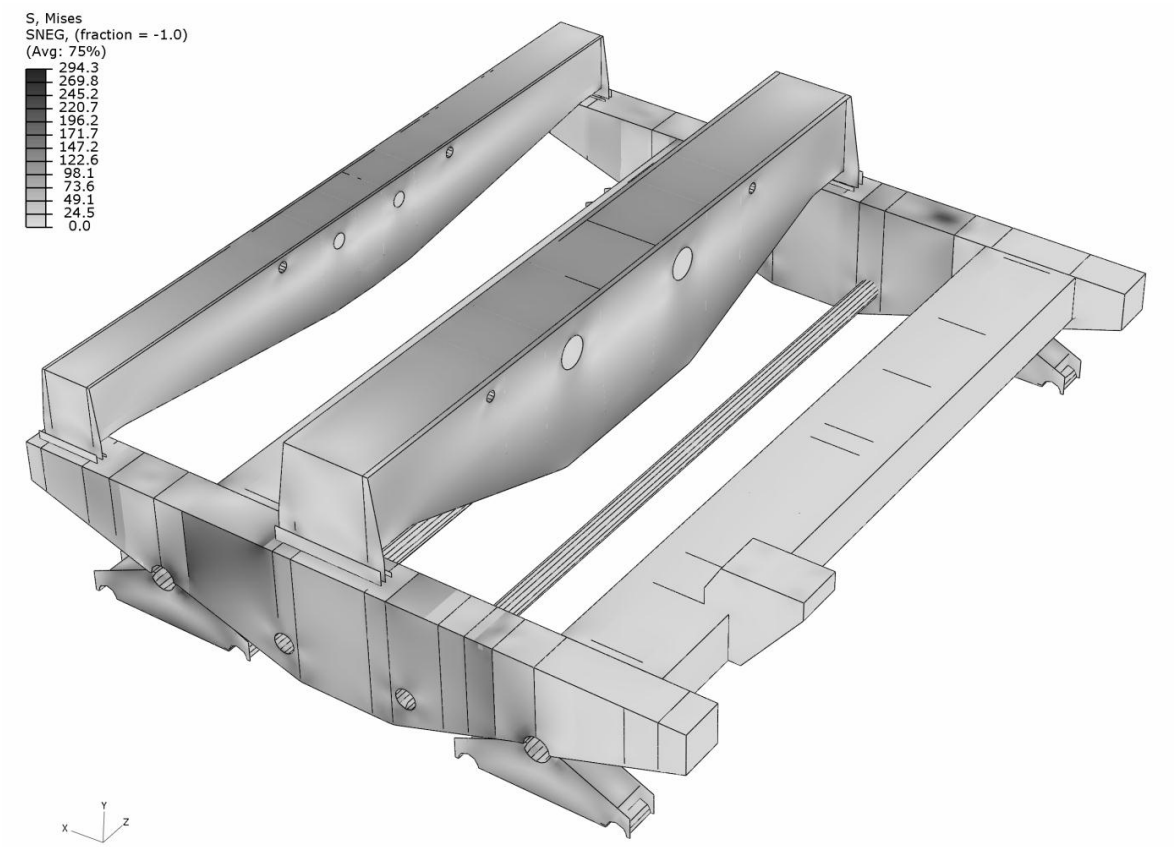

Fig. 54a. Stress in the hoisting winch structure according to Huber-Mises-Hencky theory (model C)
Rys. 54a. Mapa naprężeń konstrukcji (model C) wg teorii Hubera-Misesa-Hencky'ego

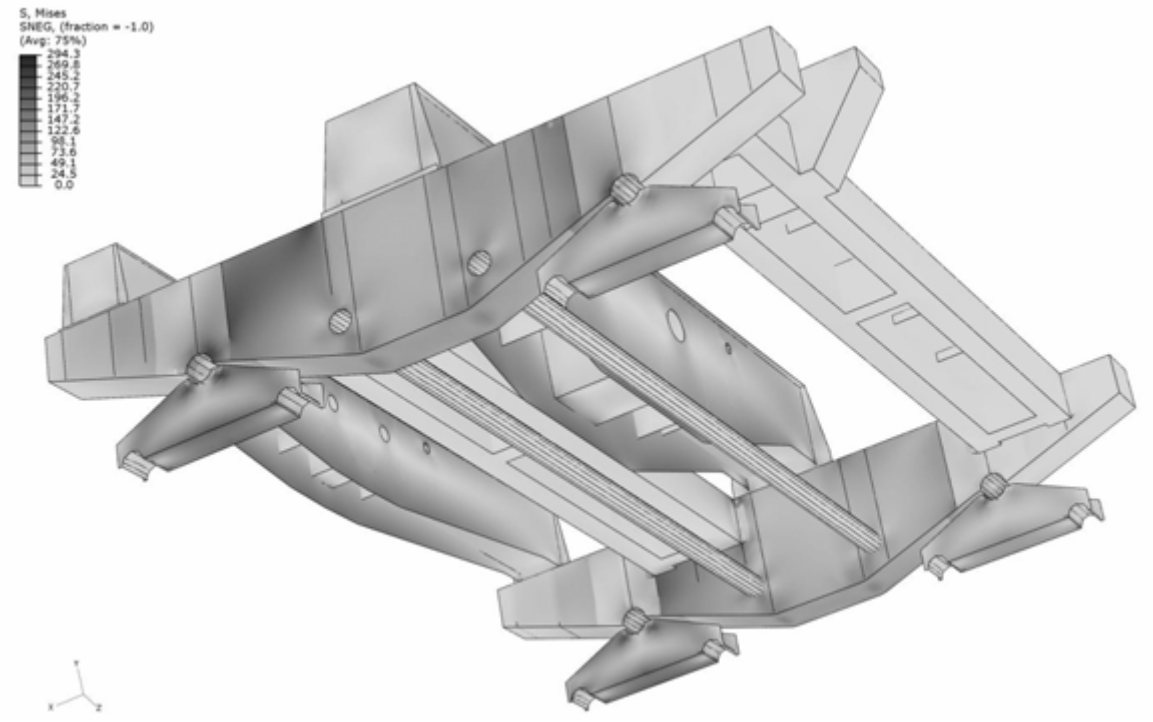

Fig. 54b. Stress in the hoisting winch structure according to Huber-Mises-Hencky theory (model C)
Rys. 54b. Mapa naprężeń konstrukcji (model C) wg teorii Hubera-Misesa-Hencky'ego

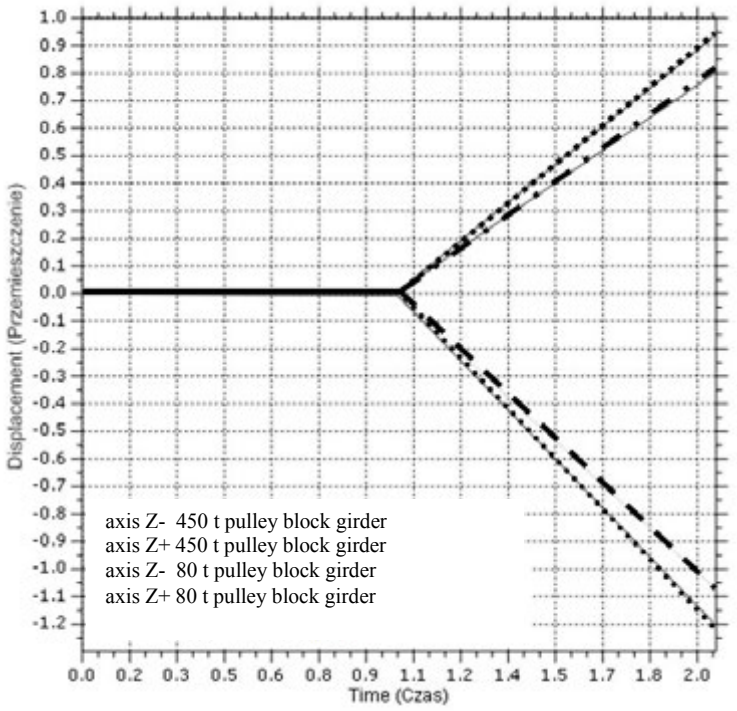

Fig. 55. Diagram showing the displacement on the girders edge, sliding on the winch's buffer beam (model C)

Rys. 55. Wykres przedstawiający przemieszczenia węzłów krawędzi dźwigara, ślizgających się po czołownicy (model C)

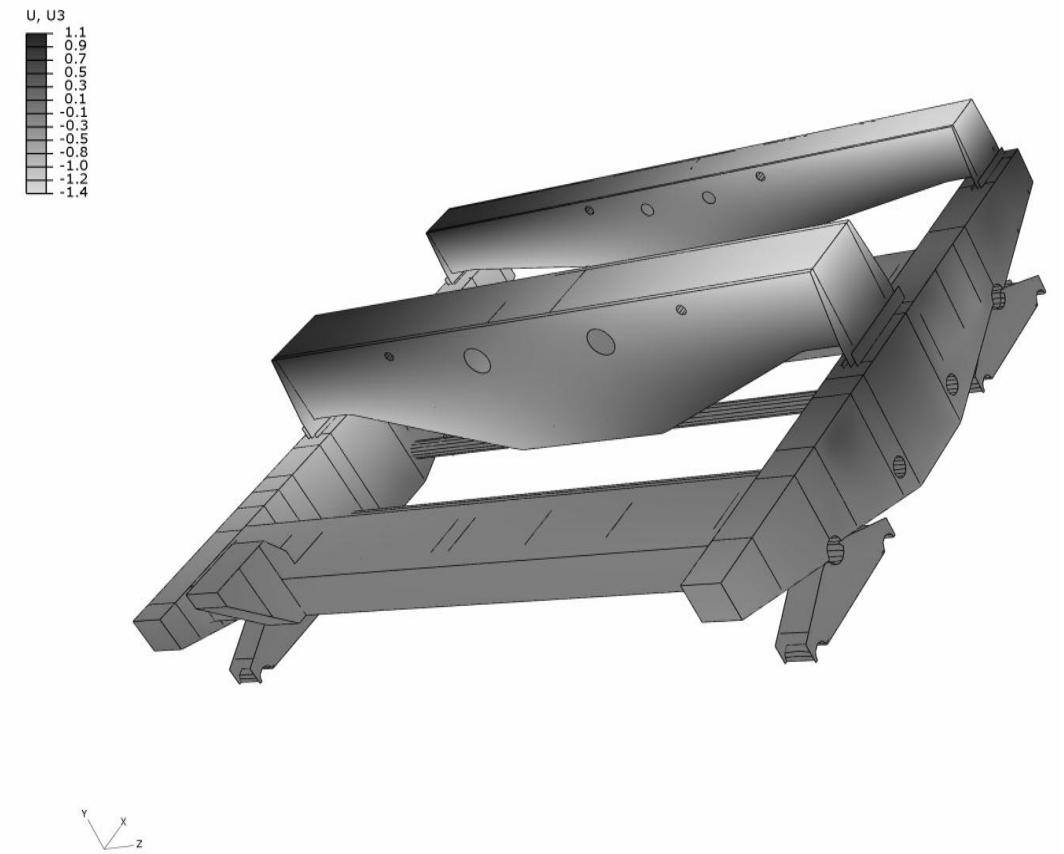

Fig. 56. Displacement in the construction of the girder on Z-axis (model C)

Rys. 56. Mapa przemieszczeń w konstrukcji w osi dźwigara (Z) (model C)

In the study also a modal analysis was made. It sets the value of the first ten natural frequencies and their forms. The fig. 57 shows the calculated winch load-carrying structure forms for the first ten frequencies.

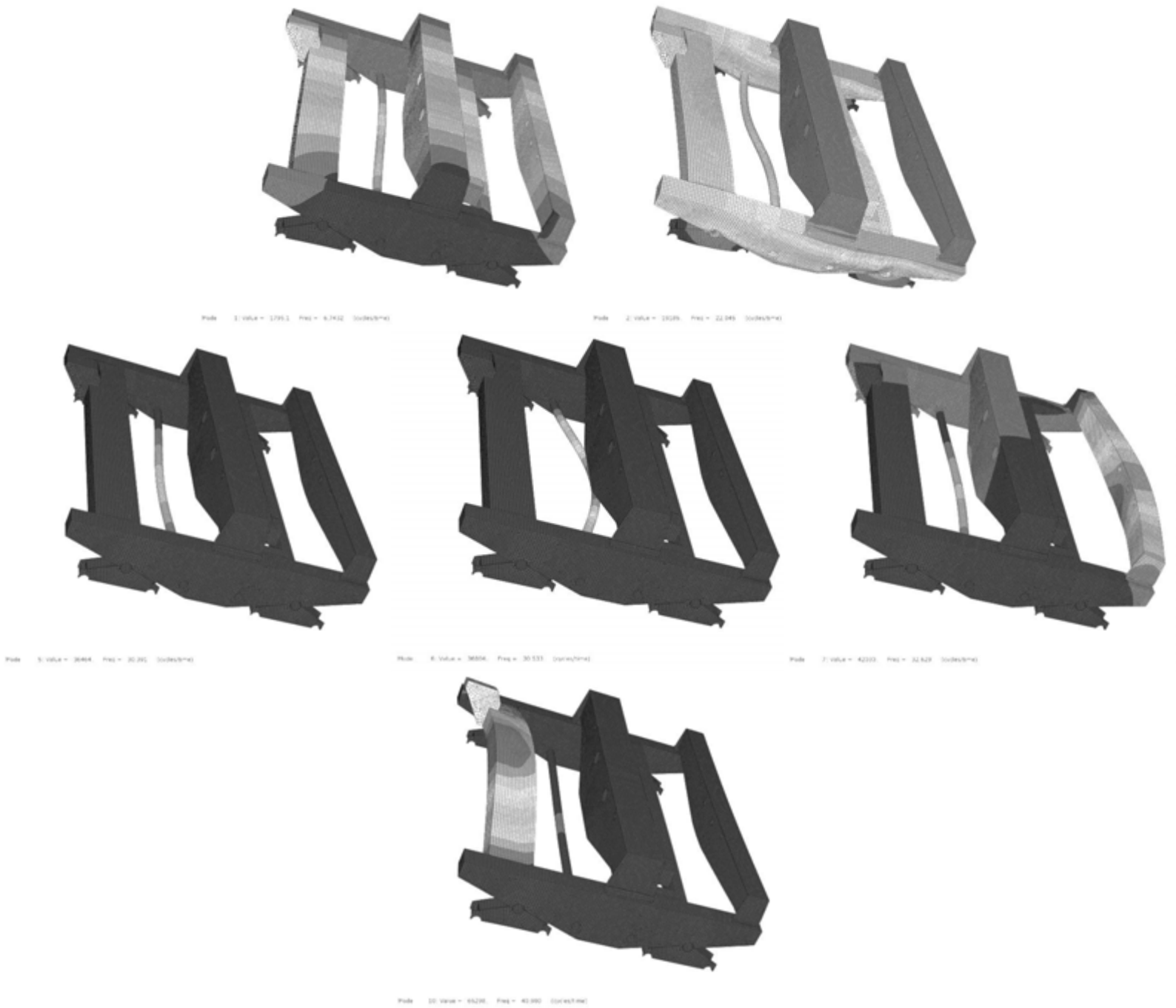

Fig. 57. Figures of natural frequencies (model A)
Rys. 57. Postacie drgań własnych (model A)

The simulations allow to make some conclusions:

1. Maximal simplified and therefore over rigid model (A) could be used only in the stage of preliminary computations of structure prototype. It is useful for determining the maximal displacement quite precisely. Local stress concentrations makes impossible the proper strength analysis of construction nodes.

2. Satisfactory and precise results through only little more preparation time needed characterize model (B). Time of computation is almost the same as in (A). higher than in reality stress values appears only between girders support and side sheet. This problem can be solved by independent computations of girders supported in pivot bearings.
3. In the case of model (C), the stress pattern in the hoisting winch structure is most similar to real ones. At the same time expenditures incurred during the modelling work and the time needed to carry out the calculations are many times higher than in variants (A) and (B). Therefore, this model can be regarded as the ultimate model for the verification "ready" form of construction. It is not needed to use such complicated model in the design phase.

REFERENCES

1. Zienkiewicz O.C.: Metoda elementów skończonych. Arkady, Warszawa 1972.
2. Autodesk, http://www.autodesk.pl/adsk/servlet/home?siteID=553660&id=760438.
3. Procad, http://www.procad.pl/pf/page/mcad/obj/85777_Autodesk_Inventor_Professional_2008,85776.html.
4. Jaskulski A.: Autodesk Inventor®10PL/10+. PWN, Warszawa 2006.
5. Dokumentacja Programu Autodesk Inventor, 2008.
6. Haniszewski T., Matyja T.: Problemy modelowania konstrukcji powłokowych z wykorzystaniem CAD, MES. VI sesja naukowa, Katowice 2008 – materiały konferencyjne (CD).
7. Piątkiewicz A., Sobolski R.: Dźwignice. WNT, Warszawa 1979.
8. Akademickie centrum komputerowe CYFRONET AGH. MSC/NASTRAN, http://www.cyf-kr.edu.pl/uslugi_obliczeniowe/?a=nastran.
9. Chodacki J., Szpytko J.: Laboratorium urządzeń dźwignicowych. AGH, Kraków 1994.
10. Misiek K., Gąska D.: Badanie wytrzymałości nowego typu członu powtarzalnego długiego przenośnika taśmowego w PGE KWB „BEŁCHATÓW" S.A. VIII Studencka Sesja Naukowa, Wydział Transportu Politechniki Śląskiej, Katowice (CD).
11. Bała M., Sładkowski A.: Opracowanie blokady wieszaka windy D5. VIII Studencka Sesja Naukowa, Wydział Transportu Politechniki Śląskiej, Katowice (CD).
12. Sładkowski A.: Accuracy Analysis of the Solution of Spatial Contact Problem by means of the FEM. „Mechanika". 2005, No. 3 (53), p. 17-21.
13. Dudziński Z., Kizyn M.: Vadamecum gospodarki magazynowej. ODDK, Gdańsk 2002.
14. Drozd A., Sładkowski A.: Analiza i propozycja przebudowy stanowiska kompletacji nakładki słupka i okiennic w magazynie SISTEMA POLAND. VIII Studencka Sesja Naukowa, Wydział Transportu Politechniki Śląskiej, Katowice (CD).
15. Gąska D.: Numeryczno–statystyczna metoda oceny nośności i stateczności stalowych ustrojów nośnych suwnic. Praca doktorska, Politechnika Śląska, Gliwice 2007.
16. Chimiak M.: Budowa suwnic i cięgników oraz ich obsługa. KaBe, Krosno 2009.
17. Ochenduszko M., Sładkowski A.: Redukcja maksymalnych naprężeń występujących w dźwigarach bramowej suwnicy kontenerowej firmy FAMAK S.A. metodą elementów skończonych. VIII Studencka Sesja Naukowa, Wydział Transportu Politechniki Śląskiej, Katowice (CD).
18. Sładkowski A., Gąska D., Matyja T., Markusik S.: Analiza wytrzymałościowa ustroju nośnego wciągarki 450/80 ton. Praca naukowo–badawcza wykonana na zlecenie Fabryki Maszyn i Urządzeń FAMAK S.A. Politechnika Śląska, Katowice 2007.
19. Norma PN-EN 13001−2:2009. Dźwignice. Zasady projektowania. Część 2: Obciążenia.

20. Norma prEN 13001−3.1:2009. Dźwignice. Zasady projektowania. Część 3.1: Naprężenia dopuszczalne oraz sprawdzanie wytrzymałości konstrukcji stalowej.
21. Abaqus 6.9 EF1 – documentation.
22. Gąska D., Haniszewski T., Matyja T.: Wpływ założeń modelowych na stan naprężeń i przemieszczeń na przykładzie wózka suwnicy 450 ton. Konferencja „Transport Problems 2010", Kraków 2010 – materiały konferencyjne (CD).
23. Al-Mayah A., Soudki K., Plumtree A.: FEM and mathematical models of the interfacial contact behaviour of CFRP-metal couples. Composite Structures, No. 73, 2006, p. 33–40.
24. Fraštia L.: Numerical solution of elastic bodies in contact by FEM utilising equilibrium displacement fields. Comput. Mech., No. 41, 2007, p. 159–174.
25. Wu J-J.: Finite element analysis and vibration testing of a three-dimensional crane structure. Measurement, No. 39, 2006, pp.740–749.
26. Matyja T., Sładkowski A.: Modeling of the Lift Crane Vibration Caused by the Lifting Loads. Zdvihací Zařízení v Teorii a Praxi, Brno 2007, p. 98-105.
27. Chmurawa M., Gąska D.: Modeling of bridge cranes for dimensioning needs of their load-carrying structures. The International Journal of INGENIUM 2005 (4). Cracow – Glasgow – Radom 2005, p. 409-414.
28. Gąska D., Matyja T., Sładkowski A., Markusik S.: Strength analysis of hoisting winch 450/80 t. Silesian University of Technology, research work, Katowice 2007, p. 67.
29. Franke D., Düster A., Nübel V., Rank E.: A comparison of the h-, p-, hp-, and rp-version of the FEM for the solution of the 2D Hertzian contact problem. Comput. Mech., No. 45 2010, p. 513–522.